# Austrian Journal of Technical and Natural Sciences

№ 9 – 10 2022
September – October

PREMIER
Publishing

Vienna
2022

# Austrian Journal of Technical and Natural Sciences

Scientific journal

№ 9 – 10 2022 (September – October)

ISSN 2310-5607



**Editorial office** Premier Publishing
Praha 8 – Karlín, Lyčkovo nám. 508/7, PSČ 18600

**E-mail:** pub@ppublishing.org

**Homepage:** ppublishing.org

**Austrian Journal of Technical and Natural Sciences** is an international, German/English/Russian language, peer-reviewed journal. It is published bi-monthly with circulation of 1000 copies.

The decisive criterion for accepting a manuscript for publication is scientific quality. All research articles published in this journal have undergone a rigorous peer review. Based on initial screening by the editors, each paper is anonymized and reviewed by at least two anonymous referees. Recommending the articles for publishing, the reviewers confirm that in their opinion the submitted article contains important or new scientific results.

Premier Publishing is not responsible for the stylistic content of the article. The responsibility for the stylistic content lies on an author of an article.

Instructions for authors

Full instructions for manuscript preparation and submission can be found through the Premier Publishing home page at:
http://ppublishing.org.

Material disclaimer

The opinions expressed in the conference proceedings do not necessarily reflect those of the Premier Publishing, the editor, the editorial board, or the organization to which the authors are affiliated.

Premier Publishing is not responsible for the stylistic content of the article. The responsibility for the stylistic content lies on an author of an article.

Included to the open access repositories:



Typeset in Berling by Ziegler Buchdruckerei, Linz, Austria.
Printed by Premier Publishing, Vienna, Austria on acid-free paper.

# Section 1. Medical science

**https://doi.org/10.29013/AJT-22-9.10-3-10**

*Wenqi Gao,*
*Westtown School, PA*

## DOES MEDICAL MARIJUANA LEGALIZATION AFFECT ADOLESCENT MARIJUANA USE?

**Abstract**

***Objective:*** Pennsylvania State legalized medical use of cannabis in year 2016. This study aims to examine if the medical marijuana legalization (MML) has any impact on adolescent marijuana use.

***Methods:*** Data from the Youth Risk Behavior Surveillance System (YRBSS) were used. Data of the states of PA and VA in years 2015 and 2017 were used. For PA, year 2015 and 2017 are pre- and post-MML, respectively. VA state was included for comparison purpose as marijuana remained illegal in VA through 2015 to 2017. Propensity score matching (PSM) was employed, to select participants from two states that are similar in key demographic characteristics. Using the matched participants, Difference-in-differences (DID) analysis was performed to compare the changes in marijuana use rate between the two states from 2015 to 2017.

***Results:*** there were some differences between two states in age and race/ethnicity before matching in both study years. PSM has improved the balance of both variables. using the matched samples, marijuana use remained stable in both states. DID analysis indicates that there's no difference in marijuana use rate change between the two states, which further means that there's no impact of medical marijuana legalization on marijuana use.

***Conclusion:*** Using matched data from YBRS, we found that the medical marijuana legalization in Pennsylvania did not have negative impact on adolescents' marijuana use.

**Keywords:** medical marijuana legalization, adolescent marijuana use, comparative analysis, Difference-in-differences analysis, propensity score matching.

**Introduction**

Although the federal government still strictly prohibits marijuana, there have been changes in many states in regulations on pot. According to Wikipedia as of May 2019, the medical use of cannabis is legal (with a doctor's recommendation) in 33 states, and recreational use of cannabis is legal in 10 states [1].

On the other hand, there has been arguments against legalizing marijuana or loosening of cannabis laws. One of the most common arguments is that it may encourage teen use of marijuana.

In Pennsylvania State, medical use of cannabis was legalized in 2016 through a bill enacted by the state legislature. In this study, we aimed to assess the impact of medical marijuana legalization (MML) in

Pennsylvania State on adolescent marijuana use, by comparing change from year 2015 to 2017, with the state of Virginia.

**Methods**

***Data source***

Data from the Youth Risk Behavior Surveillance System (YRBSS) were used. (https://www.cdc.gov/healthyyouth/data/yrbs/index.htm)

YRBSS was developed in 1990 by the Centers for Disease Control and Prevention (CDC), aiming to monitor health-related behaviors that contribute to deaths and disabilities among youth and adults. It includes national, state, territorial, tribal government, and local school-based surveys of representative samples of students in 9th through 12th grade. These surveys are conducted every two years.

YRBSS monitors six categories of health-related behaviors:

- Behaviors that contribute to unintentional injuries and violence;
- Sexual behaviors related to unintended pregnancy and sexually transmitted diseases, including HIV infection;
- Alcohol and other drug use;
- Tobacco use;
- Unhealthy dietary behaviors;
- Inadequate physical activity.

This study used combined states data conducted by departments of health and education, which provide data representative of mostly public high school students in each jurisdiction.

Data of the states of PA and VA in years 2015 and 2017 were used. For PA, year 2015 and 2017 are pre- and post-MML, respectively. VA state was included for comparison purpose. It is a neighbor to PA geographically. More importantly, marijuana remained illegal in VA through 2015 to 2017. Therefore, by including VA as the comparison group, the study will be able to detect the effect of marijuana legalization in PA from any effect explained by other variables that influence the secular trend.

***Definition of Outcome***

In YRBS, Students were asked "During the past 30 days, how many times did you use marijuana?". Answers were:

A. 0 times B. 1 or 2 times C. 3 to 9 times D. 10 to 19 times E. 20 to 39 times F. 40 or more times

A variable "current marijuana use" was created, with current marijuana use =1 if students chose B, C, D, E, or F, and current marijuana use =0 if students chose A.

***Data analysis***

**Step 1. propensity score matching (PSM)**

There is some differences between the two states in terms of population size and composition in terms of age, race/ethnicity etc. [2]. Therefore, propensity score matching (PSM) was employed, to select participants from two states that are similar in key demographic characteristics. PSM is a statistical matching technique that attempts to balance two groups accounting for characteristics/covariates that are related to the group assignment (which, in this case, is state of residence).

In this study, PSM was performed for years 2015 and 2017 separately, using logistic regression model. In the model, "state" is the outcome variable, and explanatory variables included the following:

- Age;
- Gender;
- Grade;
- Race/ethnicity;
- Smoking;
- Drinking.

From the logistic model, a propensity score was calculated for every subject. Then matching was performed to match individuals based on the exact values of the score. We also assessed if the PSM was successful by comparing the distribution of the propensity score and Standardized Mean Differences (SMD) between the two states.

**Step 2. Analysis based on the matched sample**

Using the matched participants, marijuana use rates of the two states were calculated for years 2015

and 2017, respectively. Difference-in-differences (DID) analysis was performed to compare the changes in marijuana use rate between the two states from 2015 to 2017. DID is a statistical technique commonly used in econometrics and quantitative research. It is intended to mitigate the effects of selection bias (i.e., differences between two comparison groups) and extraneous factors [3]. In this study, to conduct DID analysis, an interaction term of state*year was included in logistic model [4]. The coefficient for the interaction is the differences-in-differences estimator. A significance level of alpha < 0.05(2-sided) is used for all analyses.

**Results**

***Propensity Score matching results***

**Overall matching results:**

The sample sizes before and after matching are summarized in (table 1).

Table 1.

| | | Virginia | Pennsylvania |
|---|---|---|---|
| 2015 | All | 1889 | 1088 |
| | Matched | 1088 | 1088 |
| | Unmatched/Discarded | 801 | 0 |
| 2017 | All | 1716 | 1224 |
| | Matched | 1220 | 1220 |
| | Unmatched/Discarded | 496 | 4 |

To assess if the matching worked, we plotted the distribution of the propensity scores between the two states both before and after matching. We also used Standardized Mean Differences (SMD) as a balance measure of the two groups. A large SMD indicates that groups are different from one another for reliable comparison [5]. Some guidelines indicate that a SMD of 0.1 or 0.25 can be a reasonable cut-off for standardized biases [5].

**Matching effect of year 2015 data:**

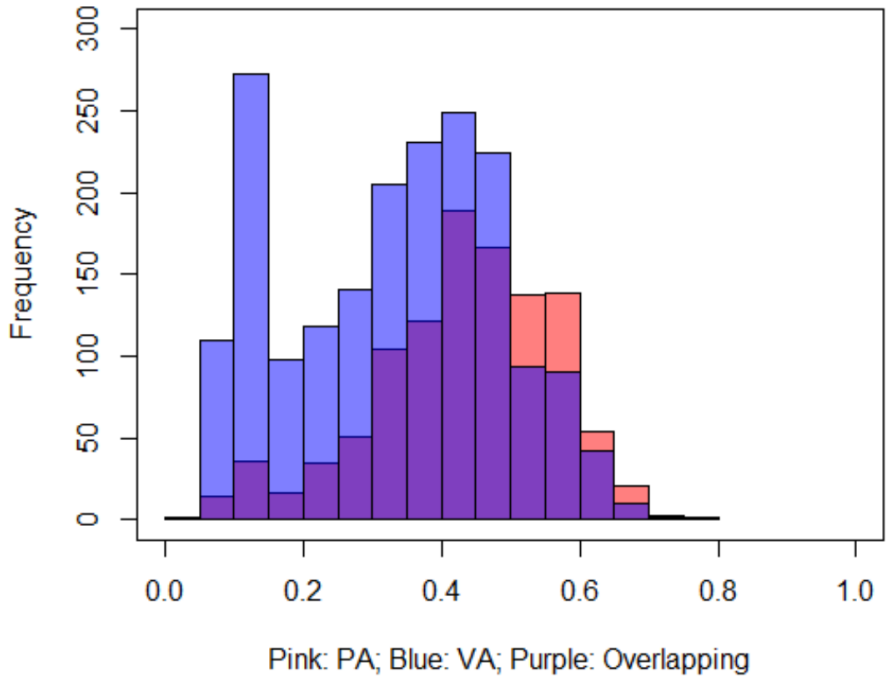


Figure 1. Propensity scores of year 2015, before matching

SMD for 2015, before matching

| | VA | PA | SMD |
|---|---|---|---|
| n | 1889 | 1088 | |
| age_cat (%) | | | 0.314 |
| 12-14 | 154 ( 8.2) | 63 ( 5.8) | |
| 15 | 356 (18.8) | 117 (10.8) | |
| 16 | 583 (30.9) | 389 (35.8) | |
| 17 | 626 (33.1) | 348 (32.0) | |
| 18 | 170 ( 9.0) | 171 (15.7) | |
| male (mean (sd)) | 0.53 (0.50) | 0.51 (0.50) | 0.035 |
| grade (mean (sd)) | 10.86 (1.01) | 10.95 (0.96) | 0.100 |
| smoking (mean (sd)) | 0.14 (0.35) | 0.13 (0.34) | 0.027 |
| drinking (mean (sd)) | 0.33 (0.47) | 0.38 (0.48) | 0.104 |
| race_ethnicity (%) | | | 0.586 |
| Black | 530 (28.1) | 82 ( 7.5) | |
| Hispanic/Latino | 249 (13.2) | 157 (14.4) | |
| Others | 187 ( 9.9) | 88 ( 8.1) | |
| White | 923 (48.9) | 761 (69.9) | |

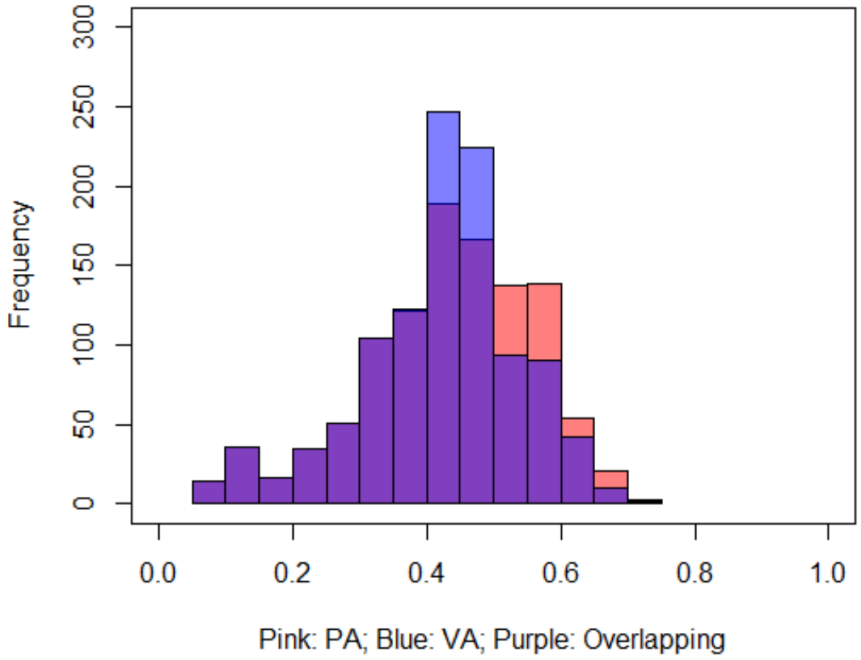


Figure 2. Propensity scores of year 2015, after matching

SMD for 2015, after matching

| | VA | PA | SMD |
|---|---|---|---|
| n | 1088 | 1088 | |
| age_cat (%) | | | 0.139 |
| 12-14 | 85 ( 7.8) | 63 ( 5.8) | |
| 15 | 121 (11.1) | 117 (10.8) | |
| 16 | 398 (36.6) | 389 (35.8) | |
| 17 | 358 (32.9) | 348 (32.0) | |
| 18 | 126 (11.6) | 171 (15.7) | |
| male (mean (sd)) | 0.51 (0.50) | 0.51 (0.50) | 0.009 |
| grade (mean (sd)) | 10.90 (1.00) | 10.95 (0.96) | 0.056 |
| smoking (mean (sd)) | 0.12 (0.32) | 0.13 (0.34) | 0.031 |
| drinking (mean (sd)) | 0.36 (0.48) | 0.38 (0.48) | 0.040 |
| race_ethnicity (%) | | | 0.067 |
| Black | 82 ( 7.5) | 82 ( 7.5) | |
| Hispanic/Latino | 181 (16.6) | 157 (14.4) | |
| Others | 93 ( 8.5) | 88 ( 8.1) | |
| White | 732 (67.3) | 761 (69.9) | |

It can be seen that, in year 2015, there were large differences between two states in age and race/ethnicity (SMD >0.25). PSM has improved the balance of both variables with lower SMDs after matching. For example:

- Distribution of age: Before matching, there were 9% of 18-year-old in Virginia versus 15.7% in Pennsylvania. After matching, the proportion difference was reduced.
- Distribution of race/ethnicity: Before matching, there were 28% of Black Americans in Virginia versus only 7.5% in Pennsylvania. After matching, the proportion difference was balanced to 7.5% of Black Americans in both states.

**Matching effect of year 2017 data:**

Similar pattern of improvement was seen for year 2017 as that in year 2015. Before matching, there were big difference in race and moderate difference in race/ethnicity. PSM improved SMDs in both of these variables.

SMD before matching:

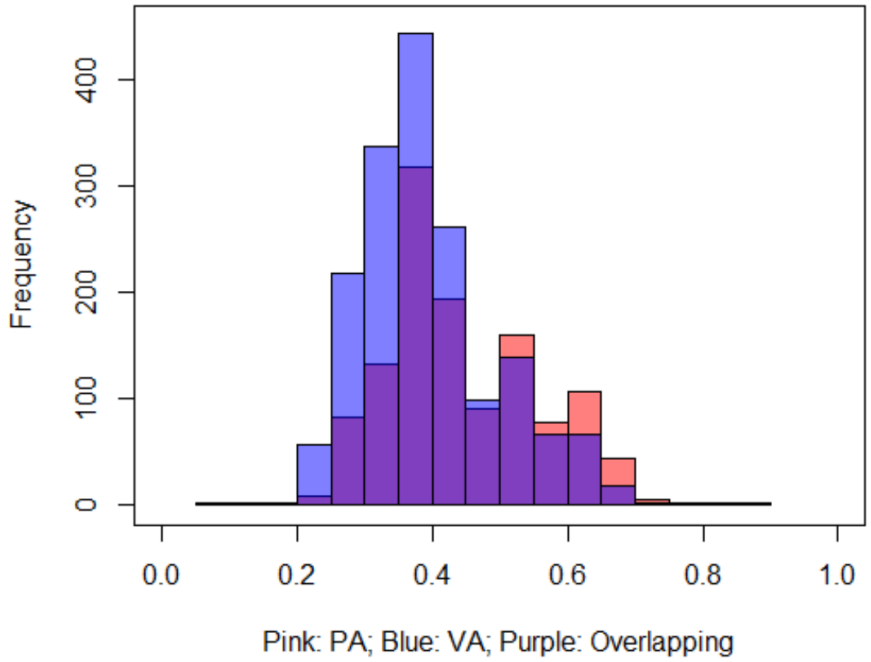


Figure 3. Propensity scores of year 2017, before matching

SMD for 2017, before matching

| | VA | PA | SMD |
|---|---|---|---|
| n | 1716 | 1224 | |
| age_cat (%) | | | 0.311 |
| 12-14 | 131 ( 7.6) | 81 ( 6.6) | |
| 15 | 308 (17.9) | 147 (12.0) | |
| 16 | 546 (31.8) | 383 (31.3) | |
| 17 | 608 (35.4) | 416 (34.0) | |
| 18 | 123 ( 7.2) | 197 (16.1) | |
| male (mean (sd)) | 0.50 (0.50) | 0.49 (0.50) | 0.003 |
| grade (mean (sd)) | 10.88 (0.99) | 10.92 (1.03) | 0.033 |
| smoking (mean (sd)) | 0.07 (0.26) | 0.09 (0.28) | 0.057 |
| drinking (mean (sd)) | 0.30 (0.46) | 0.35 (0.48) | 0.105 |
| race_ethnicity (%) | | | 0.203 |
| Black | 268 (15.6) | 160 (13.1) | |
| Hispanic/Latino | 303 (17.7) | 218 (17.8) | |
| Others | 254 (14.8) | 114 ( 9.3) | |
| White | 891 (51.9) | 732 (59.8) | |

SMD after matching:

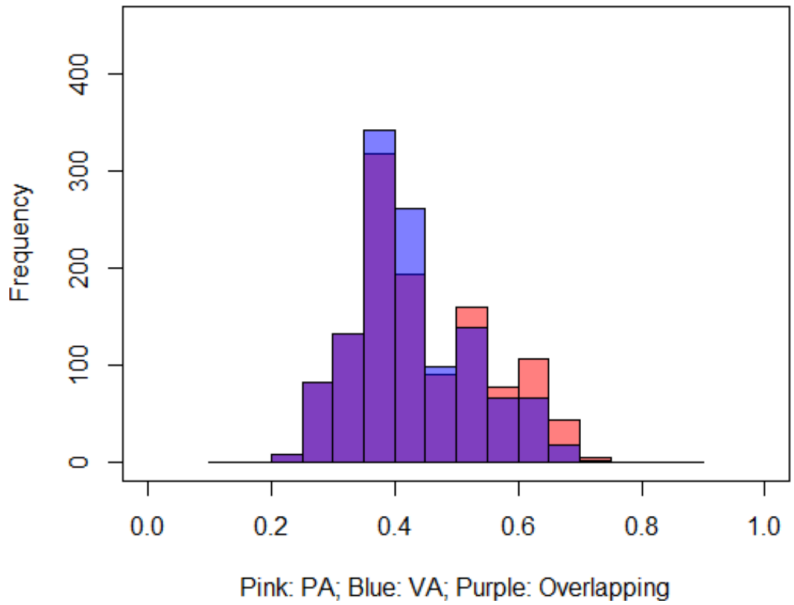


Figure 4. Propensity scores of year 2017, after matching

SMD for 2017, after matching

| | VA | PA | SMD |
|---|---|---|---|
| n | 1220 | 1220 | |
| age_cat (%) | | | 0.225 |
| 12-14 | 98 ( 8.0) | 78 ( 6.4) | |
| 15 | 113 ( 9.3) | 147 (12.0) | |
| 16 | 435 (35.7) | 383 (31.4) | |
| 17 | 455 (37.3) | 416 (34.1) | |
| 18 | 119 ( 9.8) | 196 (16.1) | |
| male (mean (sd)) | 0.50 (0.50) | 0.49 (0.50) | 0.023 |
| grade (mean (sd)) | 10.92 (1.00) | 10.91 (1.03) | 0.002 |
| smoking (mean (sd)) | 0.08 (0.27) | 0.09 (0.28) | 0.024 |
| drinking (mean (sd)) | 0.35 (0.48) | 0.35 (0.48) | 0.003 |
| race_ethnicity (%) | | | 0.027 |
| Black | 156 (12.8) | 160 (13.1) | |
| Hispanic/Latino | 222 (18.2) | 217 (17.8) | |
| Others | 104 ( 8.5) | 112 ( 9.2) | |
| White | 738 (60.5) | 731 (59.9) | |

***Marijuana use rates***

From unmatched data, it seemed that adolescents' marijuana slightly increased in PA while slightly decreased in VA. However, using the matched samples, marijuana use remained stable in both states, and the trend seemed to be very similar.

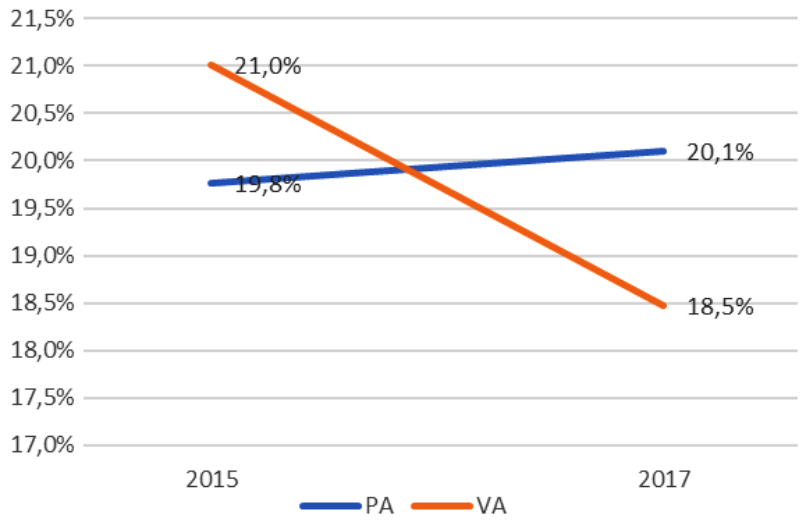


Figure 5. Marijuana use rate before matching

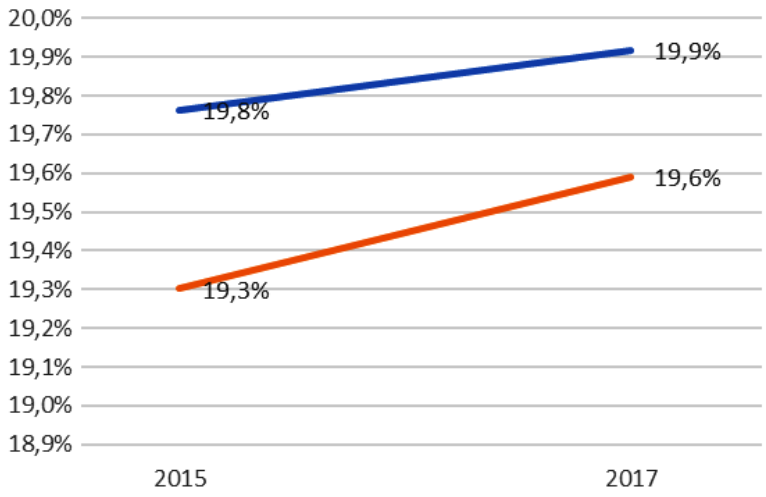


Figure 6. Marijuana use rate before matching

***Impact of medical marijuana legalization on marijuana use: results from DID analysis***

As mentioned above, when testing the impact of medical marijuana legalization on marijuana use using DID analysis, the metric to look for is the interaction term between state and year.

```
Coefficients:
                          Estimate Std. Error z value             Pr(>|z|)
(Intercept)              -1.401298   0.076136 -18.405 <0.0000000000000002 ***
sitecodeVA               -0.029242   0.108155  -0.270                0.787
as.factor(year)2017       0.009872   0.104572   0.094                0.925
sitecodeVA:year 2017     -0.001882   0.148570  -0.013                0.990
```

The P-value of the interaction term of state*year was 0.99. This indicates that there's no difference in marijuana use rate change between the two states, which further means that there's no impact of medical marijuana legalization on marijuana use.

**Discussion**

In this study, we specifically examined if the medical marijuana legalization had any impact on adolescents' marijuana use. In order to make a fair comparison, we used Virginia as control group, so that any other factors at the same time as the MML such as other policy changes are taken into account. Virginia is a good control option since marijuana has remained illegal through the study years. Meanwhile, these two states are close geographically.

We did notice that there are demographic differences between these two states, mainly in age and race/ethnicity. By employing propensity score matching, we were able to select comparison groups that are better balanced in key demographic characteristics. From the matched samples, marijuana use rates in both states remained stable from year 2015 to 2017. From the DID analysis, we found no difference in the marijuana use change between the two states. Therefore, it can be argued that the medical marijuana legalization in Pennsylvania did not negatively impact the marijuana use of the state.

This is consistent with findings from other states. For example, a federal report reveals that teen marijuana use in Colorado did not increase since adult use marijuana was legalized in 2012 [6]. Meanwhile, a state-run survey of 37.000 middle and high school students in Washington state finds that rates of marijuana use among adolescents have remained virtually flat **since** the state legalized recreational marijuana in 2012 [7]. A lot of data showed that not only does legalization not increase teen marijuana use, but also the loosening of cannabis laws doesn't make it any easier for teens to access marijuana. Nor does it influence their attitudes toward marijuana [6].

According to the Marijuana Policy Project spokesperson Mason Tvert, "… it should be particularly welcome news for those who opposed the state's legalization for fear it would lead to an explosion in teen use. Hopefully it will allay opponents' concerns in other states where voters or lawmakers are considering proposals to legalize and regulate marijuana for adult use" [6].

Our findings added one more piece to the evidence of no negative effect of MML on adolescent marijuana use. Like Mason Tvert stated, " Rather than debating whether marijuana should be legal for adults, let's focus on how we can regulate it and control it to make it less available to teens" [6].

**Summary**

Using matched data from YBRS, we found that the medical marijuana legalization in Pennsylvania did not have negative impact on adolescents' marijuana use.

## References:


1. Legality of cannabis by U.S. jurisdiction. Wikipedia Available at: URL: https://en.wikipedia.org/wiki/Legality_of_cannabis_by_U.S._jurisdiction
2. Pennsylvania vs. Virginia: state comparisons. Index Mundi Available at: URL: https://www.indexmundi.com/facts/united-states/quick-facts/compare/pennsylvania.virginia
3. Abadie A. Semiparametric Difference-in-Differences Estimators. Rev. Econ. Stud.– 75. 2005.
4. Torres-Reyna O. Differences-in-Differences (using R). (2015).
5. Stuart E. A., Lee B. K. & Leacy F. P. Prognostic score-based balance measures can be a useful diagnostic for propensity score methods in comparative effectiveness research. J. Clin. Epidemiol.– 66. 2013.– P. 84–90. e1.
6. No increase in teen marijuana use in colorado post-legalization, federal government reports. Medical marijuana inc., news available at: URL: https://news.medicalmarijuanainc.com/teen-marijuana-colorado
7. Cvdvt.org. Washington State Survey Shows Youth Marijuana Use Unchanged Since Legalization. (2017). Available at: URL: https://www.cvdvt.org/washington-state-survey-shows-youth-marijuana-use-unchanged-since-legalization
8. Focus on Health and Safety of Gaming Hospitality Workforce. American Nonsmokers' Rights Foundation Available at: URL: https://no-smoke.org/at-risk-places/casinos

**https://doi.org/10.29013/AJT-22-9.10-11-17**

*Normuradova Nodira M.,*
*Center for the Development of Professional Qualifications of Medical Workers, Tashkent, Uzbekistan*

# DOPPLER ASSESSMENT OF FETAL DIASTOLIC DYSFUNCTION

**Abstract.** The article presents the results of a study of the pulmonary artery and vein in the assessment of cardiac dysfunction in fetuses with cardiomegaly. The Doppler in the artery and vein was obtained in one control volume. Acceleration time (AT), ejection time (ET), isovolumic contraction time (IVCT), isovolumic relaxation time (IVRT), duration of the A wave (Adur), atrial contraction time (ACT), the max velocity in the PV at the moment of opening of the atrioventricular valve (at point AVO), the max velocity in the PV in ventricular systole (at point S) and AVO/S, AT/ET, ACT/IVRT, IVRT/ET were also calculated. In diastolic dysfunction, there was a shortening IVRT, lengthening of the atrial time, and a decrease in the AVO/S ratio. Systolic dysfunction of the heart was characterized by a pronounced dicrotic notch in the arterial spectrum, a decrease in the wave after the closure of the semilunar valve/or retrograde blood flow in the ventricular diastole.

**Keywords:** diastolic dysfunction, fetus, Doppler sonography, pulmonary artery, pulmonary vein.

In recent years, many researchers have increasingly paid attention to the assessment of cardiac dysfunction in fetuses: methods such as Speckle tracking echocardiography are used, which have great prospects due to the possibility of obtaining measurements of longitudinal, radial and transverse deformation of the myocardium, Tissue Doppler (TDI), magnetic resonance imaging [1; 2]. However, unfortunately, there are still limitations in the widespread availability of these methods in the health care system.

Dopplerography is a relatively in expensive, accessible and non-invasive method in the diagnosis of myocardial dysfunction. To date, to assess global cardiac dysfunction in children and adults, including fetuses, the calculation of the MPI index (myocardial performance index) is widely used [3]. An analysis of the literature data on the use of the MPI index in fetuses showed a large scatter of the data obtained [4–6], which are apparently related to the technical aspects of the measurements. The development of new, effective, accessible, and easily reproducible methods for assessing fetal cardiac dysfunction is undoubtedly an urgent task of prenatal diagnosis. Our approach to the diagnosis of fetal cardiac dysfunction is based on the assessment of the Doppler spectrum of blood flow in the pulmonary arteries and veins.

**Material and methods**

In a prospective study, the main group included 69 pregnant women (5 patients with multiple pregnancies) who were observed at the Republican Scientific and Practical Center for Obstetrics and Gynecology of the Ministry of Health of the Republic of Uzbekistan, with a pathology of the heart in the fetus. A total of 74 fetuses were studied, including 51 fetuses (group 1) with cardiomegaly of various origins (CHD, FGR, fetal edema, hemolytic anemia of the fetus, twin-twin transfusion syndrome, diabetic macrosomia) and 23 fetuses with CHD without cardiomegaly (group 2). The control group consisted of 63 patients without extragenital pathology and with 10 to 70, on average 36.5 ± 6.5 percentile. Ultrasound examinations were carried out on Samsung WS80A (Korea) expert-class devices using convex probes with a frequency of 3.5–5 MHz.

All fetuses underwent standard fetometry, including biparietal head size, head and abdomen circumference, and thigh length. Cardio – femoral index (the ratio of the width of the heart at the level of the atrioventricular valves to the length of the thigh) was used to assess cardiomegaly, and Color Doppler mapping (CD) was used to study intracardiac hemodynamics. In all fetuses, when scanning through a four-chamber section, the pulmonary veins were removed, while the control volume of the spectral Doppler was set to capture both the pulmonary vein and the pulmonary artery. Using spectral doppler graph, the following parameters were measured: acceleration time (AT, acceleration time) and ejection time (ET, ejection time) in LA, isovolumic contraction time (IVCT), isovolumic relaxation time (IVRT, isovolumic relaxation time), duration of the A-wave in the PV spectrum (A dur, duration of the A wave), atrial contraction time (ACT), maximum velocity in the PV at the time of opening of the atrioventricular valve (at the AVO point, atrioventricular valve opening), maximum velocity in the PV in ventricular systole (at point S, systole) (Fig. 1), and also calculated such indicators as the ratio of velocity in the pulmonary artery at the moment of opening of the atrioventricular valve to the maximum velocity in ventricular systole AVO/S, the ratio of acceleration time to ejection time AT/ET, the ratio of atrial contraction time to isovolumetric relaxation time ACT/IVRT, and the ratio of isovolumetric relaxation time relaxation by IVRT/ET ejection time. Statistical data were calculated using the Statistics 23 program. The data of the first and second groups were compared with the control group, the differences in the groups were considered statistically significant at $p < 0.05$.

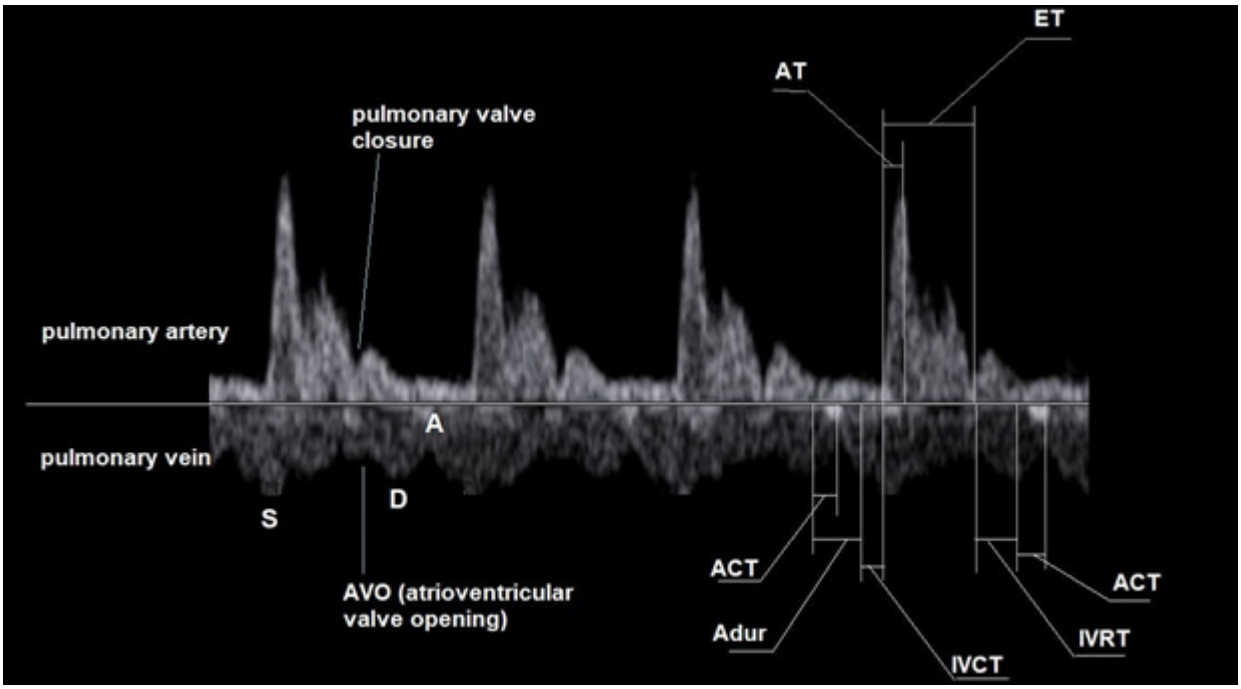


Figure 1. Doppler spectrum of blood flow in the pulmonary artery (above the isoline) and pulmonary vein (below the isoline)

**Results**

The indicators of gestational age of the first group were 28.2 ± 3.0, in the second group 26.04 ± 4.4 weeks, in the control group 29.47 ± 4.17 weeks. CFI in the control group 0.52 ± 0.02, in the first group 0.64 ± 0.04, in the second group 0.50 ± 0.01.

The mean value of AT in the first group was 33.0 ± ± 2.6 ($p < 0.05$), in the second group 30.2 ± 1.7 ($p = = 0.55$), in the control group 29.9 ± 1.9; ET – 180.0 ± ± 8.9 ($p < 0.05$), 175.6 ± 8.4 ($p = 0.90$), 175.9 ± 11.9; IVCT – 41.8 ± 4.0 ($p < 0.05$), 30.3 ± 7.5 ($p = 0.56$), 31.6 ± 8.3; IVRT – 72.7 ± 11.1 ($p < 0.05$), 82.0 ±

± 3.0 (p > 0.05), 84.1 ± 7.7; A dur 169.9 ± 30.0 (p < < 0.05), 163.8 ± 21.3 (p = 0.17), 157.6 ± 19.7; AST – 92.6 ± 11.4 (p < 0.01), 67.0 ± 5.7 (p< 0.05), 74.0 ± ± 16.2; AVO – 9.7±2.7 (p < 0.05), 12.0 ± 3.1 (p = = 0.79), 12.5 ± 3.2; S – 25.6 ± 3.6 (p < 0.05), 21.0 ± ± 4.2 (p = 0.81), 20.7 ± 3.2, respectively (table 1–3).

We also evaluated IVRT/ET, AST/IVRT ratios to assess diastolic dysfunction of the heart. The mean values of IVRT/ET in the first group were 0.41 ± ± 0.17 (CI 68% 0.24–0.58), in the second group 0.47 ± ± 0.03 (CI 95% 0.40–0.54), in the control group 0.48 ± 0.08 (95% CI 0.40–0.54), p-values for the first group compared with the control group were p < 0.01 (there are statistically significant differences between these groups), for the second group p = 0.12. For the ACT/IVRT indicator, the mean values in the first group were 1.32 ± 0.3 (CI 68% 0.68–1.95), in the second group 0.82 ± 0.09 in the control group – 0.90 ± 0.2 (95% CI 0.37–1.42), p<0.01 for the first group, p > 0.05 for the second group.

The presence of cardiomegaly in hemolytic anemia in the fetus was accompanied by changes in the spectrum of the pulmonary vein, caused by diastolic dysfunction (Fig. 2), there was a decrease in the ratio of the velocity at the point of opening of the atrioventricular valve to the maximum velocity during ventricular diastole AVO/S0.31 ± 0.03 with CI 95% of the control group 0.42–0.74. Atrial time A dur was also increased by 207.3 ± 11.1 ms (CI 95% of the control group 109–205 ms). IVRT/ET and AST/IVRT ratios were within 95% CI of the control group – 0.53 ± ± 0.03 (0.40–0.54) and 1.11±0.17 (0.37–1.42), respectively, despite the fact that the indicators of ACT 118.8 ± 17.6 ms (36–112 ms), IVRT 107.8 ± 5.4 ms (62–105 ms) and ET 206.7 ± 18.6 ms (146–205 ms) were higher than the values of the control group. The AT/ET ratio was increased to 0.22 ± 0.01 (95% CI 0.15–0.19 control group) (table 1–3). The group with fetal growth retardation had a wide range of values. In cases of an early form of IGR, there was a decrease in the IVCT value, an increase in the IVRT, AST and A dur values, while AT, ET corresponded to the values of the control group. The spectrum of the pulmonary vein in the late form of IGR showed shortening of IVRT, ET, AST and lengthening of A dur. The AT values had a spread from 23 ms to 57 ms, averaging 33.1 ± ± 5.3 ms (24.2–34.7). The mean ET in this subgroup was 166.3±18.9 ms (146–205 ms), IVCT 39 ± 5.5 ms (9.4–54.3 ms), IVRT 74.6±16.4 ms (62 .4–105.8 ms), ACT 90.5 ± 24.9 ms (36–112 ms). In diabetic macrosomia, a normal spectrum of the pulmonary artery and vein was recorded, with only a slight deviation in the indicators of the systolic function of the heart – an increase in the AT/ET ratio, apparently due to volume overload. Mild valvular regurgitation was noted in the pulmonary valve. The mean value in the group with diabetic macrosomia was AT 30.4 ± 1.1 ms (24.2–34.7), ET 192 ± 9.2 ms (146–205 ms), IVCT 45.7 ± 4.0 ms (9.4–54.3 ms), IVRT 70.7 ± 16.4 ms (62.4–105.8 ms), ACT 90.5 ± 24.9 ms (36–112 ms). In fetuses with a large weight for gestational age, in the absence of diabetes in a woman, systolic AT function and the AT/ET ratio were increased, indicating volume overload of the heart during macrosomia. The spectrum of the umbilical artery, ductus venosus, and middle cerebral artery were within normal limits.

Diastolic dysfunction of the heart in fetuses with twin-twin transfusion syndrome was also manifested by an increase in atrial time, acceleration time, and a decrease in isovolumetric contraction time. Changes in the parameters of the pulmonary vein AT, ET, IVST, IVRT correlated with CFI. With fetal edema (pronounced hydrothorax), if the CFI was not increased, then the spectrum of the pulmonary vein and artery remained normal (Fig. 3). In the venous duct, there was an increase in the pulsatile index PI 0.84 with CFI 0.49. The spectrum of the pulmonary artery and vein indicated the absence of cardiac dysfunction: IVRT / ET 0.52 (95% CI of the control group 0.40–0.54), AST / IVRT 0.64 (95% CI of the control group 0.37–1.42), AVO/S0.52 (95% CI of control group 0.42–0.74), AT/ET 0.19 (95% CI of control group 0.15–0.19).

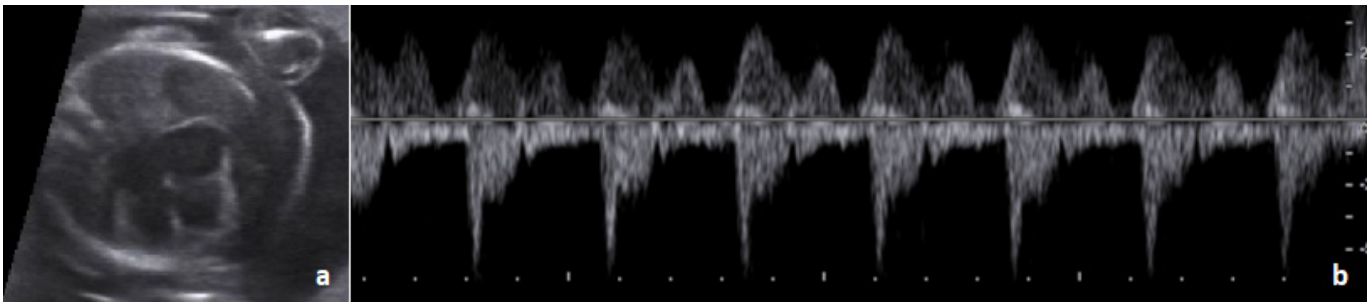


Figure 2. Diastolic dysfunction in a fetus with hemolytic anemia at 35 weeks of gestation, cardiomegaly (CFI 0.65). In the spectrum of the pulmonary vein (above the isoline), there was a decrease in the ratio of the velocity at the point of opening of the atrioventricular valve to the maximum velocity during ventricular diastole AVO/S0.25 (0.42–0.74) and an increase in atrial time A dur 207 ms (109–205 ms). a) cardiomegaly b) Doppler spectrum of pulmonary artery and vein

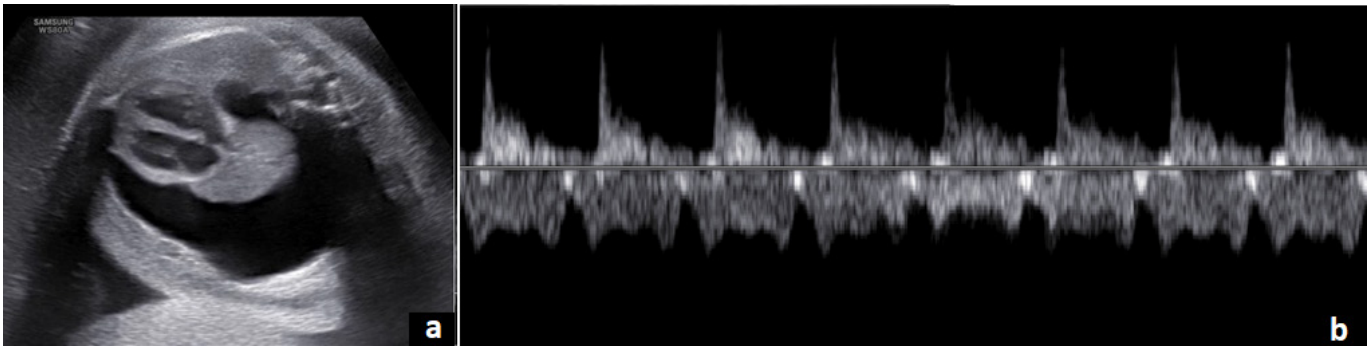


Figure 3. Doppler spectrum of blood flow in the pulmonary artery (above the isoline) and vein (below the isoline) in a fetus of 30 weeks of gestation with severe idiopathic hydrothorax, without cardiomegaly. The spectrum of the pulmonary vein is normal

**Discussion**

The proposed method for assessing cardiac dysfunction is based on obtaining the blood flow of the pulmonary artery and vein in the same spectrum. Technically, this is easy to do, since the pulmonary veins in the area of confluence with the left atrium are located next to the pulmonary arteries. In a four-chamber section, it is necessary to bring out the pulmonary veins on one side and capture the pulmonary vein together with the pulmonary artery into the control volume. Normal spectra of the pulmonary artery and vein in the second and third trimesters are shown in Figure 4.

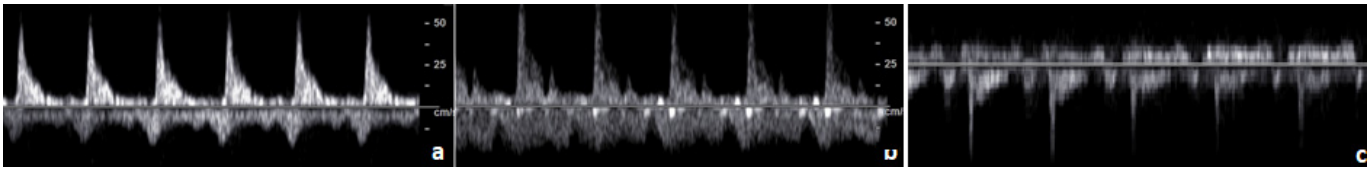


Figure 4. Spectrum of the pulmonary artery and vein at 20 weeks (a) and 37 weeks (b) of gestation during normal pregnancy. In the third trimester of pregnancy in the spectrum of the pulmonary artery, the closing point of the pulmonary valve and the antegrade wave following it become more pronounced due to the elasticity of the vessel walls. Reverse in the pulmonary vein (c) in a fetus of 19 weeks of gestation with a normal course of pregnancy

Using the spectrum of the pulmonary artery and vein, we estimated the **M**PI (myocardial performance index). The time of isovolumetric relaxation was calculated from the point of opening of the atrioventricu-

Table 1.– Comparison of mean values of AT, ET, IVCT, IVRT in the pulmonary artery and vein in the first and control groups

| | AT, ms | | | ET, ms | | | IVCT, ms | | | IVRT, ms | | |
|---|---|---|---|---|---|---|---|---|---|---|---|---|
| | First group | Control group | p-value | First group | Control group | p-value | First group | Control group | p-value | First group | Control group | p-value |
| CHD, n=11 | 33.2±5.0 | 29.9±2.6 | p>0.05 | 170.0±11.4 | 175.9±11.9 | p>0.05 | 41.8±3.4 | 31.6±8.3 | p>0.05 | 83.6±5.3 | 84.1±10.8 | p>0.05 |
| Early FGR, n=13 | 33.15±8.8 | 29.9±2.6 | p>0.05 | 166.3±16.9 | 175.9±11.9 | p>0.05 | 39.0±7.3 | 31.6±8.3 | p>0.05 | 74.6±21.3 | 84.1±10.8 | p>0.05 |
| Fetal edema (not immune), n=3 | 33.0±3.6 | 29.9±2.6 | p>0.05 | 191.3±25.7 | 175.9±11.9 | p>0.05 | 43.6±1.1 | 31.6±8.3 | p>0.05 | 102.3±7.6 | 84.1±10.8 | p>0.05 |
| Fetal hemolytic anemia, n=7 | 43.8±6.7 | 29.9±2.6 | p<0.05* | 206.7±30.1 | 175.9±11.9 | p<0.05* | 43.7±14.9 | 31.6±8.3 | p>0.05 | 107.8±7.7 | 84.1±10.8 | p<0.05* |
| TTTS donor, n=5 | 33.0±1.0 | 29.9±2.6 | p>0.05 | 177.6±6.2 | 175.9±11.9 | p>0.05 | 41.8±6.8 | 31.6±8.3 | p>0.05 | 87.0±3.3 | 84.1±10.8 | |
| TTTS recipient, n=5 | 31.6±1.8 | 29.9±2.6 | p>0.05 | 179.2±8.9 | 175.9±11.9 | p>0.05 | 41.8±7.2 | 31.6±8.3 | p>0.05 | 57.2±2.1 | 84.1±10.8 | p<0.05* |
| Diabetic macrosomia, n=7 | 30.4±1.6 | 29.9±2.6 | p>0.05 | 192.4±11.1 | 175.9±11.9 | p>0.05 | 45.7±5.7 | 31.6±8.3 | p>0.05 | 70.7±1.7 | 84.1±10.8 | p>0.05 |

*p < 0.05* there are statistically significant differences*

*AT: acceleration time, ET: ejection time, IVCT: isovolumic contraction time, IVRT: isovolumic relaxation time*

Table 2.– Comparison of mean values of ACT, Adur, AVO, S in the pulmonary artery and vein in the first and control groups

| | ACT, ms | | | A dur, ms | | | AVO, cm/sec | | | S, cm/sec | | |
|---|---|---|---|---|---|---|---|---|---|---|---|---|
| | First group | Control group | p-value | First group | Control group | p-value | First group | Control group | p-value | First group | Control group | p-value |
| *1* | *2* | *3* | *4* | *5* | *6* | *7* | *8* | *9* | *10* | *11* | *12* | *13* |
| CHD, n=11 | 157.4±23.6 | 157.6±19.7 | p>0.05 | 75.2±3.8 | 74.0±16.2 | p>0.05 | 15.2±3.4 | 12.2±3.2 | p>0.05 | 29.3±3.5 | 20.7±3.2 | p<0.05* |
| Early FGR, n=13 | 167.2±29.1 | 157.6±19.7 | p>0.05 | 90.5±24.9 | 74.0±16.2 | p>0.05 | 7.8±1.4 | 12.2±3.2 | p>0.05 | 21.7±2.7 | 20.7±3.2 | p>0.05 |
| Fetal edema is not immune, n=3 | 210.6±7.1 | 157.6±19.7 | p<0.05* | 96.6±0.4 | 74.0±16.2 | p>0.05 | 7.3±0.9 | 12.2±3.2 | p>0.05 | 25.0±0.6 | 20.7±3.2 | p>0.05 |
| Fetal hemolytic anemia, n=7 | 207.3±11.1 | 157.6±19.7 | p<0.05* | 118.8±17.5 | 74.0±16.2 | p<0.05* | 8.3±1.2 | 12.2±3.2 | p>0.05 | 27.0±3.2 | 20.7±3.2 | p>0.05 |

| *1* | *2* | *3* | *4* | *5* | *6* | *7* | *8* | *9* | *10* | *11* | *12* | *13* |
|---|---|---|---|---|---|---|---|---|---|---|---|---|
| FFTS donor, n=5 | 176.0±4.0 | 157.6±19.7 | p>0.05 | 106.4±10.4 | 74.0±16.2 | p<0.05* | 8.6±1.4 | 12.2±3.2 | p>0.05 | 23.6±2.2 | 20.7±3.2 | p>0.05 |
| FFTS recipient, n=5 | 207.8±8.1 | 157.6±19.7 | p<0.05* | 98.4±3.6 | 74.0±16.2 | p>0.05 | 9.0±1.2 | 12.2±3.2 | p>0.05 | 28.8±3.7 | 20.7±3.2 | p<0.05* |
| Diabetic macrosomia, n=7 | 157.4±23.6 | 157.6±19.7 | p>0.05 | 75.2±3.8 | 74.0±16.2 | p>0.05 | 15.2±3.4 | 12.2±3.2 | p>0.05 | 29.3±3.5 | 20.7±3.2 | p<0.05* |

*p < 0.05* there are statistically significant differences*

*ACT: atrial contraction time, A dur: duration of A wave, AVO: atrioventricular opening, S: systole*

Table 3.– Comparison of the average ratios of IVRT/ET, AST/IVRT, AVO/S, AT/ET in the pulmonary artery and vein in the first and control groups

| | **IVRT/ET** | | | **ACT/IVRT** | | | **AVO/S** | | | **AT/ET** | | |
|---|---|---|---|---|---|---|---|---|---|---|---|---|
| | **First group** | **Control group** | **p-value** | **First group** | **Control group** | **p-value** | **First group** | **Control group** | **p-value** | **First group** | **Control group** | **p-value** |
| CHD, n=11 | 0.49±0.02 | 0.48±0.08 | p>0.05 | 0.90±0.10 | 0.90±0.26 | p>0.05 | 0.51±0.08 | 0.58±0.08 | p>0.05 | 0.19±0.03 | 0.17±0.02 | p>0.05 |
| Early FGR, n=13 | 0.45±0.14 | 0.48±0.08 | p>0.05 | 1.12±0.26 | 0.90±0.26 | p>0.05 | 0.35±0.05 | 0.58±0.08 | p<0.05* | 0.20±0.05 | 0.17±0.02 | p>0.05 |
| Fetal edema is not immune, n=3 | 0.54±0.09 | 0.48±0.08 | p>0.05 | 0.95±0.07 | 0.90±0.26 | p>0.05 | 0.29±0.04 | 0.58±0.08 | p<0.05* | 0.18±0.04 | 0.17±0.02 | p>0.05 |
| Fetal hemolytic anemia, n=7 | 0.53±0.08 | 0.48±0.08 | p>0.05 | 1.11±0.21 | 0.90±0.26 | p>0.05 | 0.31±0.03 | 0.58±0.08 | p<0.05* | 0.22±0.09 | 0.17±0.02 | p<0.05* |
| FFTS donor, n=5 | 0.49±0.02 | 0.48±0.08 | p>0.05 | 1.23±0.19 | 0.90±0.26 | p>0.05 | 0.36±0.05 | 0.58±0.08 | p<0.05* | 0.19±0.01 | 0.17±0.02 | p>0.05 |
| FFTS recipient, n=5 | 0.31±0.01 | 0.48±0.08 | p<0.05* | 1.72±0.10 | 0.90±0.26 | p<0.05* | 0.31±0.02 | 0.58±0.08 | p<0.05* | 0.17±0.01 | 0.17±0.02 | p>0.05 |
| Diabetic macrosomia, n=7 | 0.36±0.01 | 0.48±0.08 | p>0.05 | 1.35±0.11 | 0.90±0.26 | p<0.05* | 0.32±0.02 | 0.58±0.08 | p<0.05* | 0.15±0.01 | 0.17±0.02 | p>0.05 |

*p<0.05* there are statistically significant differences*

lar valve in the venous spectrum (or the closing of the semilunar valve in the arterial spectrum) to point D, the start point of atrial contraction. When calculating the isovolumetric contraction, the ejection onset point was considered as the end point, and certain difficulties arose when determining the IVCT reference point, since it was difficult to accurately determine the time of closing of the atrioventricular valve on the spectrum. As you can see in (Fig. 1), A point is clearly visible on the spectrum, the end of atrial contraction, then the atrium relaxes and an antegrade blood flow begins in the pulmonary vein, which accelerates to the beginning of systole. Hypothetically, we took half the time from point A "end of atrial systole" to the point of the start of ejection time in the arterial spectrum (or point S in the venous spectrum).

In the first group, the MPI index averaged 0.65 ± ± 0.11 with a 95% CI 0.43–0.87, in the second group it was 0.64 ± 0.06 (95% CI 0.50–0, 78) and in the control group 0.66 ± 0.10 (95% CI 0.45––0.87), when comparing both groups with the control $p > 0.05$, no statistically significant difference was found. This is apparently due to the heterogeneity of the group with cardiomegaly, which included fetuses with growth retardation, diabetic fetopathy, immune and non-immune edema, etc. To clarify the data, studies in a homogeneous group are required. We have demonstrated that IVCT, IVRT and ET measurements can easily be obtained using the spectrum in the pulmonary artery and vein.

Thus, the data of our study showed that diastolic dysfunction can be judged by the shortening of the time of isovolumetric myocardial contraction, the lengthening of the atrial time, and the decrease in the AVO/S ratio. Systolic dysfunction of the heart was characterized by a pronounced dicrotic notch in the spectrum, a decrease in the wave after the closure of the semilunar valve/or retrograde blood flow in the ventricular diastole.

Our results allow us to state that the study of the Doppler spectrum of blood flow in the pulmonary artery and vein (in a single control volume) makes it possible to assess the presence and nature of cardiac dysfunction in fetuses with cardiomegaly.

## References:


1. De Vore G.R., Klas B., Satou G., Sklansky M. Longitudinal Annular Systolic Displacement Compared to Global Strain in Normal Fetal Heart sand Those With Cardiac Abnormalities. J. Ultrasound Med.– 37: 2018.– P. 1159–1171.
2. Buryakova S. I., Medvedev M. V., Strupeneva U. A., Nikolaeva E. V. Evaluation of the contractile function of the fetal myocardium in obstructive lesions of the aorta. Prenatal diagnosis.– 19(3): 2020.– P. 220–227.
3. Tei C., Ling L. H., Hodge D. O. New index of combined systolic and diastolic myocardial performance: a study in normals and dilated cardiomyopathy. J Cardiol.– 26(6): 1995.– P. 357–366.
4. Friedman D., Buyon J., Kim M., Glickstein J. S. Fetal cardiac function assessed by Doppler myocardial performance index (Tei Index). Ultrasound Obstet Gynecol.– 21(1): 2003.– P. 33–36.
5. Ghawi H., Gendi S., Mallula K., Zghouzi M., Faza N., Awad S. Fetal left and right ventricle myocardial performance index: defining normal values for the second and third trimesters – single tertiary center experience. pediatric cardiology.– 34(8): 2013.– P. 1808–1815.
6. Tsutsumi T., Ishii M., Eto G., Hota M., Kato H. Serial evaluation for myocardial performance in fetuses and neonates using a new Doppler Index. Pediatric Int.– 41:1999.– P. 722–727.

# Section 2. Food processing industry

**https://doi.org/10.29013/AJT-22-9.10-18-21**

*Akhmedov Azimjon Normuminovich,*
*Doctor of Technical Sciences, Professor*
*of the Department of Food Technology of Products*
*of the Karshi Engineering and Economic Institute, Karshi, Uzbekistan*

*Atakulova Dilfuza Tursunovna,*
*Associate Professor of the Department of Food Technology*
*of Products of the Karshi Engineering and Economic Institute,*
*Karshi, Uzbekistan*

*Kholmurodova Zubayda Diyorovna,*
*Associate Professor of the Department of Food Technology*
*of Products of the Karshi Engineering and Economic Institute,*
*Karshi, Uzbekistan*

*Shaymardonova Gulmira Xudoynazarovna,*
*3 rd year student of Karshi Institute of Engineering*
*and Economics, Food Technology, Karshi, Uzbekistan*

## ANALYSIS OF CHLOROPHYLLS IN LOW QUALITY COTTONSEED OIL

**Abstract.** This scientific article presents information about the effect of increasing the amount of cotton seed pods on the quality of cotton oils obtained from I–IV cotton seeds. In particular, in the processing of low-grade cotton seed in JSC "Karshi oil-extraction", the pulpiness of the pulp is 4.3–6.0% higher than the usual one, or the degree of crushing of the pulp obtained from low-grade cottonseed is 5.5–6, 5 percent higher. With the introduction of reverse goods, cottonseed bolls are partially reduced, but this has been shown to be insufficient to significantly reduce the bolls of the pressed material.

The color of low-quality cottonseed oil was found to be 20–21 red units higher than the color of ordinary (I–II grades) cottonseed oil by 7–8 blue units. Particular attention should be paid to the difference in pigments in the blue units that condense the processes of cleaning the obtained oils with alkali and bleaching with activated adsorbents.

**Keywords:** chlorophyll, alkali, blue units, red units, cotton seeds, cotton oils, JSC "Karshi yog-extraction", JSC "Koson oil-extraction".

**Introduction**

The main task of the oil industry of the Republic of Uzbekistan is to produce environmentally friendly, competitive, high-quality products for the population. Training of qualified personnel is of great importance in performing this task. Oil processing technology includes a number of production processes. Among them, the most important are oil refining, hydrogenation, production of margarine and margarine products, mayonnaise, fatty acids, glycerin and soap.

During the production of cottonseed oil, dark-colored crude oils are more often obtained, where, along with gossypol and its derivatives, pigments of chlorophyll and its derivatives are present [1, p. 23–26].

The content of chlorophyll and its derivatives in crude oils depends on the conditions of their extraction and the maturity of cotton seeds.

When chlorophyll is treated with alkali, colorless substances are not formed, which must be borne in mind when choosing an industrial method for bleaching vegetable oils containing a significant amount of chlorophyll.

$$C_{32}H_{30}ON_4Mg\begin{cases}COOCH_3\\COOC_{20}H_{39}\end{cases}\xrightarrow{Alkali}C_{32}H_{30}ON_4Mg\begin{cases}COOH\\COOH\end{cases}+\begin{matrix}CH_3OH\\C_{20}H_{39}OH\end{matrix}$$

*Chlorophyll a* *Chlorophyllin a* *Phytol*

$$C_{32}H_{28}O_2N_4Mg\begin{cases}COOCH_3\\COOC_{20}H_{39}\end{cases}\xrightarrow{Alkali}C_{32}H_{28}O_2N_4Mg\begin{cases}COOH\\COOH\end{cases}+\begin{matrix}CH_3OH\\C_{20}H_{39}OH\end{matrix}$$

*Chlorophyll to* *Chlorophyllin to* *Phytol*

When chlorophyll is treated with acids, magnesium is split off from its molecule. The acute action of acids leads to the formation of pheophytin a and pheophytin b. It is assumed that it is the presence of pheophytins that is the reason for the green color of vegetable oils.

There is a close relationship between the rancidity of oils and their chlorophyll content. Chlorophyll can act as a photosensitizer when oils are exposed to light. According to [2, p. 11–16], chlorophyll in the light is a stimulator of oxidation, while in the absence of light it does not affect the oxidative process. The accelerating effect of chlorophyll on the oxidative rancidity of fats is delayed by the addition of antioxidants.

In the presence of phenolic oxidation inhibitors, chlorophyll is a positive synergist. However, when illuminated, it exhibits negative synergism.

Partially, chlorophyll is removed from oils during alkaline refining and more completely when they are treated with natural sorbents. The color intensity of oils can be significantly weakened by the action of solar radiation and $\gamma$-radiation. $\gamma$-radiation is especially effective, which opens up the possibility of practical use of this method for decolorizing technical green oils.

Solutions of chlorophylls in organic solvents have characteristic absorption spectra in the region of 400–500, 600–700 nm. Therefore, the spectrophotometric method is currently one of the main methods used in the study and analytical determination of chlorophylls [3, p. 77–78].

**Materials and methods.** The article uses modern methods of chemical, physico-chemical and other analyzes with the processing of the results by statistical methods [4, p. 107].

We have studied the content of chlorophyll and its derivatives in oils obtained from ordinary (grades I and II) and low-grade (grades III and IV) cotton seeds. Sampling was carried out during the normal operation of the JSC "Karshi yog-extraction" and JSC "Koson oil-extraction". The analyzes of these samples and the resulting oil were carried out according to the "Guidelines for research methods ..." [4, p. 107].

**Results.** The results of the analysis of the content of the husk in the petal mint and pulp are presented in table 1.

From Table. Table 1 shows that at both enterprises, when processing ordinary (I–II varieties) cotton seeds, the content of husks in the petal, mint and pulp is much lower than when processing low-grade (III and IV varieties) seeds. For example, in the joint venture JSC "Karshi oil-extraction" the huskiness of the petal during the processing of low-grade cotton seeds is 4.3–6.0% higher compared to the traditional one. Or the puddleness of mint obtained from low-grade cotton seeds is higher by 5.5–6.5% compared to the usual one. With the introduction of reverse goods, the huskiness of the pulp is partially reduced, but this is not enough to significantly reduce the husk content in the pressed material.

Table 1.– Changes in the content of husks (huskiness) in the petal, mint and pulp obtained from ordinary (I–II varieties) and low-grade (III–IV varieties) cotton seeds

| Business name | Husk content (huskiness),% | | | | | |
|---|---|---|---|---|---|---|
| | when processing ordinary (I–II varieties) cotton seeds (control) | | | when processing low-grade (III and IV grades) seeds | | |
| | in a petal | in mint | in the pulp | in a petal | in mint | in the pulp |
| JSC "Karshi oil-extraction" | 12.1–12.6 | 15.0–18.7 | 13.5–14.3 | 16.4–18.6 | 21.5–24.3 | 20.1–21.5 |
| JSC "Koson oil-extraction" | 11.8–13.5 | 15.5–19.2 | 13.8–15.7 | 16.8–18.9 | 22.3–25.8 | 21.2–22.4 |

Comparison of data for two enterprises shows that when processing low-grade cotton seeds in petal, mint and pulp, the husk content (husk content) increases by about 5–7% compared to the traditional one. This negatively affects the quality of the resulting oil, in particular, increases the content of chlorophyll and its derivatives, which are presented in (table 2).

Table 2.– Change in the mass fraction of chlorophyll and its derivatives in oils obtained from ordinary and low-grade cotton seeds by pressing methods

| Business name | Mass fraction of chlorophyll and its derivatives in oils obtained from:% | |
|---|---|---|
| | when processing ordinary (I–II varieties) cotton seeds (control) | when processing low-grade (III and IV grades) seeds |
| JSC "Karshi oil-extraction" | 0.5 ÷ 0.6 | 1.1 ÷ 1.2 |
| JSC "Koson oil-extraction" | 0.6 ÷0.7 | 1.2 ÷ 1.3 |

From Table. (Table 2) shows that in oils obtained from ordinary medium-fiber cotton seeds, the mass fraction of chlorophyll and its derivatives is contained within 0.5–0.7%, and in oils obtained from low-grade cotton seeds – within 1.1–1.3%. The increased content of green pigments in the composition of raw cottonseed oil complicates the processes of its alkaline refining and bleaching with activated adsorbents.

Table 3.– Change in the color of oils obtained from ordinary and low-grade cottonseeds

| Business name | Color at 70 yellow oils obtained from: | | | |
|---|---|---|---|---|
| | conventional (I and II varieties) cotton seeds | | low-grade (III and IV grades) cotton seeds | |
| | red units | blue units | red units | blue units |
| JSC "Karshi oil-extraction" | 60.5 | 4.7 | 81.9 | 11.3 |
| JSC "Koson oil-extraction" | 63.7 | 5.5 | 85.2 | 13.7 |

Unfortunately, in practice, the content of husks in mint, pulp and others is often not regulated, due to which the color of the resulting crude oil significantly deteriorates. We confirm the data (Table 3.) obtained by measuring on a color calorimeter of the Lovibond type.

Table 3 shows that the color of oils obtained from low-grade cotton seeds is approximately 20–21 red units and 7–8 blue units higher compared to the color of oils obtained from ordinary (I–II varieties) cotton seeds. Particular attention should be paid to the difference in pigments in blue units, which condense the processes of alkaline refining of the obtained oils and their bleaching with activated adsorbents.

**Discussion and Conclusion.** Thus, summarizing the results of this study, we can state that in order to improve the processes of alkaline refining of cottonseed oils and their bleaching, it is necessary to stabilize the content of the husk in the composition of the petal, mint and pulp. At the same time, it is necessary to select the optimal amount of the return product introduced into the fryer. it also contains substances that color the resulting oil in red and blue colors.

High-temperature processing of pulp leads to the formation of new derivatives of chlorophyll with other components, which complicates subsequent processing of cottonseed oil. Therefore, in order to increase the yield and quality of the resulting oil, it is necessary to improve the processes of processing low-grade cotton seeds and obtaining oils for various purposes from them.

## References:

1. Akhmedov A. N. Investigation of indicators of cottonseed oil obtained by pre-pressing from low-grade cotton seeds // Universum: Technical Science. – Issue: 4(61). – April, 2019.– Moscow, 2019.– P. 23–26.
2. Akhmedov A. N., Abdurahimov S. A. The study of the grinding process of rushanka from the nuclei of cotton seeds of different varieties. Journal Chemistry and Chemical Engineering.– No. 3. 2018.– P. 11–16.
3. Abdurahimov S. A., Ergasheva D. K., Nazirov A. N. Spectral evaluation of the qualitative composition of refined oils. Izvestiya vuzov. Food technology,– No. 6. 1990.– P. 77–78.
4. Rzhekhin V. P. and others – L. Guidance on research methods, technochemical control and accounting of production in the oil and fat industry // Under the general editorship of prof.: VNIIZH-1967. I.– 585 p.

# Section 3. Technical sciences

**https://doi.org/10.29013/AJT-22-9.10-22-25**

*Turemuratova Alfiya Sharibaevna,*
*PhD candidate of chemistry laboratories*
*in Karakalpak Research Institute of Natural Sciences*
*of the Karakalpak Branch of the Academy of Sciences RUz, Nukus*
*Reymov Karjaubay Dauletbaevich,*
*Doctor of Technical Sciences (PhD), associate professor*
*at Nukus State Pedagogical Institute named after Ajiniyaz*
*Erkaev Aktam Ulashevich,*
*Tashkent Chemical Technological Institute*
*of the Republic of Uzbekistan, Tashkent*
*Allaniyazov Davran Orazymbetovich,*
*Doctor of Technical Sciences,*
*(PhD) Karakalpak Research Institute of Natural Sciences*
*of the Karakalpak Branch of the Academy of Sciences RUz, Nukus*

## ION-SALT COMPOSITION OF WESTERN DEEP-WATER PART OF GREAT ARAL SEA AND ITS VARIABILITY

**Abstract.** The process of draining the bottom of the Aral Sea is relative to the content of individual ions, which depends on the regions of the staged salt formations. Based on the results of the studies, measures were developed the relative content of which decreased from the dried bottom of the Aral Sea. Our drilling of the bottom of the Aral Sea showed that the thickness of soil sediments from the south to the north ranges from 2 to 6 m with a humidity of 40–80%. Salt content of groundwater was 0,4–0,9% lower compared to seawater.

Based on studies conducted to establish the distribution patterns of clay materials and soluble salts in the soil, the western shore of the Great Aral Sea was divided into three layers. In the first layer, there is no pattern of change in the observed indicators. The second and third layers separately and the relationships have certain patterns. It has been found that in the second layer, with increasing depth, the content of clay components of the soil decreases, and at the beginning of the third layer it increases again, but less than at the beginning of the second layer. These phenomena affect the distribution of soluble salts.

**Keywords:** Aral Sea, ions, reduction, sulfate-chloride, water retention, depths, soils, regularity, water-soluble salts.

**Introduction.** The Aral Sea is located within Uzbekistan and Kazakhstan in the northern part of the desert regions of Central Asia between 43°28' and 46°52' N and 58°4' and 61°56' E from Greenwich. The name "Aral Sea" – from the word "Aral" is associated with the fact that the huge basin lies on an island among the waterless deserts of the Turan lowland. The water area of the Aral Sea in the west is limited by steep chinks, an extensive plateau stretching to the Caspian Sea, the Ustyurt plateau, rising 100–200 m above the level of the Aral Sea. In the south is the flat space of the modern and ancient Amu Darya Delta, south turning into velvet sand massifs of the Zanguz Karakums. n the east it borders on Kyzylkum – a desert plain with a common slope towards the sea. In the north and north-west, the coastline of the water area is limited to the barley sands of the Mugojar foothills [1].

In connection with the beginning of an intensive decrease in the level of the Aral Sea and the emergence of the first fears about its possible complete disappearance in the future in the early 60 s, research began on the problem of the Aral Sea.

Most researchers (B. V. Andrianov, A. S. Kes, P. V. Fedorov, etc.), based on geological and historical surveys, came to the almost consensus that in prohistoric times, changes in the level and salinity of the Aral Sea occurred due to changes in the natural climate. During the humid climatic phase, the sea level reached a maximum value of 72–73 m abs, and during the arid climate, the Aral level fell, and the degree of salinity of the Aral Sea grew [2–6].

**Research objects and methods.** The object of research in this work is salt-forming ions in water, and the soil of the lowered bottom of the Aral Sea of the Muinak region.

**Research material and methodology.** Water extraction of soils was prepared according to the generally accepted method-soil: water in a ratio of 1:5 [7]. The content of chlorine ions was determined by argentometric methods by sea; calcium and magnesium trilonometric; sulfate by titration; aqueous drawing with a sulfuric acid solution in the presence of a methyl orange indicator; sodium and potassium ions by the difference in the sum of anions and cations. The results of the analysis of aqueous extracts were expressed in milligram equivalents per 100 g of dry air soil, the sum of water-soluble salts in percent.

The results of the aqueous extract analysis were monitored for a dense (dry) residue.

The degree of soil salinity was assessed on a scale of [7–9].

Table 1.– Relative contents (% by weight) of the main salt-forming ions in the water of the Great Aral Sea in 2020 and 2022

| № | Soil type | total $HCO_3$ in% | $Cl^{-}$% | $SO_4^{-}$% | $Ca^{+}$% | $Mg^{+}$% | Anions-cations mg/eq | Na+K by difference in% | Note |
|---|---|---|---|---|---|---|---|---|---|
| 1 | 25.06.20 | 4.88 | 14.2 | 168.0 | 4.008 | 23.69 | 3980/2150 | 45.75 | 170 |
| 2 | 05.12.20 | 7.32 | 14.2 | 86.4 | 7.014 | 13.36 | 2320/1450 | 21.75 | 170 |
| 3 | 05.03.21 | 4.88 | 14.2 | 122.4 | 4.008 | 20.04 | 3030/1850 | 29.5 | 160 |
| 4 | 07.07.21 | 3.66 | 10.6 | 117.6 | 5.01 | 18.22 | 2810/1750 | 26.5 | 170 |
| 5 | 08.09.21 | 4.88 | 14.2 | 91.2 | 5.01 | 15.18 | 2380/1500 | 22.0 | 170 |
| 6 | 25.02.22 | 3.66 | 10.6 | 72.0 | 4.008 | 17.61 | 1860/1650 | 5.25 | 170 |
| 7 | 07.03.22 | 4.88 | 10.6 | 72.0 | 3.006 | 20.04 | 1880/1800 | 2.0 | 180 |
| 8 | 10.05.22 | 3.66 | 21.3 | 72.0 | 3.006 | 19.44 | 2160/1750 | 10.25 | 180 |

**Research results**

It can be seen that the relative contents of individual ions before the start of sea drying and in 2020–2022 differ quite significantly. The most significant changes occurred with the $Ca_2^{+}$ ion, the relative content of which decreased. This fact is not surpris

ing, since the curing of calcium carbonate and gypsum should lead to the effective removal of calcium from the aqueous mass. The content of sulfate ion, which is also consumed during gypsum deposition, has also decreased. The content of the $Cl^-$ ion, on the contrary, has grown. Due to the last two facts, the sulfate-chloride ratio of $SO_4^{2-}/Cl^-$, considered an important characteristic of the chemical type of the reservoir, decreased by 42%. Thus, during the drying of the Aral Sea, its belonging to the class of sulfate-type reservoirs became less pronounced, and the waters of this sea to some extent approached the chloride type characteristic, in particular, of ocean waters. Also, the relative content of the $HCO_3^-$ ion consumed as a result of the carbonates was significantly reduced (by about 0.5 times).

Consistent changes in the ion-salt composition of the waters of the Great Aral Sea 2020–2022 show that in the samples of 2022, the relative calcium content was 3.006% (compared with 7.014 in 2020).

Thus, the calcium content was reduced before our eyes by the curing of minerals, and this process was quite visible, even in a relatively short observation period. This ratio should be less sensitive to the precipitation of salts in interannual time scales, since only relatively small fractions of the available mass of chloro-ion and sulfate-ion are involved in these processes, in contrast to $Ca_2^+$ and $HCO_3^-$, a significant part of which has already fallen. Also, during the analysis, the chemical compositions of soil samples obtained from the western shore of the deep-water western part of the Great Aral Sea were studied in (Table 2).

No changes in observed parameters were observed in the first layer. The indicators of the second and third layers changed according to certain patterns.

Table 2. – Chemical composition of soil samples obtained from the western shore of the deep-water western part of the Great Aral Sea

| № | Sampling date | Coordinates | | Sampling depth, cm | Dry Stock Current | total $HCO_3$ in% | $Cl^{-}$% | $SO_4^-$ % | Ca% | Mg% | Anions-cations mg/eq | Na+K by difference in% | Sum of components in% | Salinity type | pH |
|---|---|---|---|---|---|---|---|---|---|---|---|---|---|---|---|
| | | northern latitude | east longitude | | | | | | | | | | | | |
| 1 | 31.05.22 | 44°04'811 | 58°26'146 | 0–5 | 5.069 | 0.214 | 0.44 | 2.88 | 0.25 | 0.47 | 76.0/51.2 | 0.57 | 4.829 | X–C | 8.0 |
| 2 | 31.05.22 | 44°04'811 | 58°26'146 | 5–10 | 2.152 | 0.073 | 0.17 | 1.27 | 0.29 | 0.18 | 32.7/30.0 | 0.06 | 2.063 | –C- | 8.0 |
| 3 | 31.05.22 | 44°04'811 | 58°26'146 | 10–23 | 4.855 | 0.153 | 0.44 | 2.82 | 0.45 | 0.42 | 73.7/57.5 | 0.37 | 4.667 | X–C | 8.0 |
| 4 | 31.05.22 | 44°04'811 | 58°26'146 | 23–32 | 3.161 | 0.153 | 0.53 | 1.50 | 0.52 | 0.25 | 48.7/47.5 | 0.02 | 2.999 | X–C | 8.0 |
| 5 | 31.05.22 | 44°04'811 | 58°26'146 | 32–51 | 3.129 | 0.122 | 0.26 | 1.74 | 0.47 | 0.18 | 45.7/38.7 | 0.16 | 2.947 | X–C | 8.0 |
| 6 | 31.05.22 | 44°04'811 | 58°26'146 | 0–5 | 2.318 | 0.061 | 0.14 | 1.39 | 0.42 | 0.13 | 34.0/32.0 | 0.04 | 2.196 | –C- | 8.0 |
| 7 | 31.05.22 | 44°04'811 | 58°26'146 | 5–10 | 2.429 | 0.073 | 0.14 | 1.41 | 0.51 | 0.01 | 34.7/26.5 | 0.19 | 2.313 | –C- | 8.0 |
| 8 | 31.05.22 | 44°04'811 | 58°26'146 | 10–17 | 2.174 | 0.073 | 0.10 | 1.27 | 0.27 | 0.06 | 30.7/19.0 | 0.27 | 2.058 | –C- | 8.0 |
| 9 | 31.05.22 | 44°04'811 | 58°26'146 | 17–32 | 1.728 | 0.061 | 0.17 | 0.93 | 0.34 | 0.08 | 25.5/24.0 | 0.03 | 1.635 | X–C | 8.0 |
| 10 | 31.05.22 | 44°04'811 | 58°26'146 | 32–47 | 1.705 | 0.085 | 0.10 | 1.00 | 0.20 | 0.16 | 25.4/23.5 | 0.04 | 1.607 | –C- | 8.0 |
| 11 | 31.05.22 | 44°04'811 | 58°26'146 | 47–67 | 1.448 | 0.061 | 0.14 | 0.81 | 0.16 | 0.14 | 22.3/20.0 | 0.04 | 1.371 | X–C | 8.0 |

For example, with an increase in depth from 5––23 cm, the dry residue and the sum of salts and components increase, and in the third layer some indicators decrease and make $Cl^-$ 0.53–0.26%, Ca 0.52–0.47%, Mg 0.25–0.18%.

The results of analysis of samples from the fourth well show that with an increase in the depth of the section from 0 to 67 cm, the sum of salts and components in the samples increases, which means a decrease in the content of clay substances in the insoluble part of the samples. Here, as well as in other well sections, soluble salts contain mainly chlorine and sulfate ions. Thus, the compositions of water-soluble salts in soil samples from the north to the southeast of the greater Aral Sea vary from sulfate to chloride-sulfate and chloride. The soil surface is covered with wrinkled clay with large cracks 15–30 cm wide, 5–10 m long and 1.0–2.0 m deep.

**Conclusions**

Thus, mirabilite salt deposits occur on the eastern shore of the western deep-water part of the Great Aral Sea, which form in winter, and dissolve in precipitation in spring-summer.

Based on studies conducted to establish the distribution patterns of clay materials and soluble salts in the soil, the western shore of the Great Aral Sea was divided into three layers. In the first layer, there is no pattern of change in the observed indicators. The second and third layers separately and the relationships have certain patterns. It has been found that in the second layer, with increasing depth, the content of clay soil components increases, and at the beginning of the third layer, some components again decrease, but less than at the beginning of the first layer. These phenomena affect the distribution of soluble salts. By chemical and physicochemical methods of studying water-soluble salts and water-insoluble soil residue, it was established that the samples contain the following water-soluble minerals: mirabilite, tenardite, halite, blödite, cognavite, leveite, vantgoffite, pentahydrate, starkeite, sanderite and kieserite.

## References:


1. Rafikov A. A. Tetyukhin G. F. Decrease in the Aral Sea level and change in the natural conditions of the lower Amu Darya. – Tashkent, 1981.– 199 p.
2. Andrianov B. V. History of the impact of agriculture on the nature of the Aral region // Izv. AN.– Ser. – No. 4. 1991.– P. 47–61.
3. The Great Aral Sea at the beginning of the 20th! centuries: physics, biology, chemistry / P. O. Zavyalov, E. G. Arashkevich, I. Bastida, etc.; Institute of Oceanology named after P. P. Shirshov RAN. – M.: Science, 2012.– 229 p.
4. Kes A. S. Palaeography of the Aral Sea in the Late Pleistocene // Paleogeography of the Caspian and Aral Seas in the Cenozoic.– 4.2. 1983.– 97106 p.
5. Fedorov P. V. Some issues of paleogeography of the Caspian and Aral in the late Pliocene and Pleistocene // Paleogeography of the Caspian and Aral Seas in the Cenozoic.– 4.1. 1983.
6. URL: http://www.oceanology.ru/aral-sea-shallow
7. Arinushkina E. V. Manual on chemical analysis of soils.– M.: Moscow State University Publishing House, 1970.– 257 p.
8. Henkel P. A. Plant physiology.– M.: Enlightenment, 1975.– P. 140–208.
9. Kovda V. A. Problems of combating desertification and salinization of irrigated soils.– M.: Kolos, 1984.– 304 p.

# Section 4. Physics

https://doi.org/10.29013/AJT-22-9.10-26-30

*Ataubayeva Akkumis Berisbayevna,*
*Berdah Karakalpak State University, Nukus, Uzbekistan*

## ON BEHAVIOR OF INTERPHASE INTERACTIONS IN SILICON CONTACT STRUCTURES DUE TO QUICK THERMAL TREATMENT

**Abstract.** The author has studied how an ohmic contact between $TiB_x$ and heavily doped silicon is shaped. As it has been shown, a low-resistance Au-Ti-TiBx-Ti-n+-Si ohmic contact is conventionally formed by its deposition on an n+-Si-substrate heated to 150 °C. The experiment reveals that quick thermal treatment (QTT) at T = 400 °C does not practically affect properties of Au-Ti-$TiB_x$-Ti-$n^+$-Si ohmic contacts, whereas QTT at T = 600 °C helps shape a kind of a $TiSi_2$– phase and leads to an increase in the value of $\rho_c$ in comparison with both the original sample and thermally heated (at T = = 400 °C) sample. Diffusion barriers based on Ti and $TiB_x$ appear heat-resistant in the range of temperatures to 600 °C.

**Keywords:** ohmic contact, boride of titan, diffusion barrier, rapid thermal annealing.

**Introduction**

As more and more microelectronics devices over lately are designed to operate in ultra-high frequency band applications, thus the role of stable metal-semiconductor ohmic contacts becomes immense in ensuring their reliable and effective operation.

To slow down or eliminate altogether degradation processes stemming from mixing in the contact-forming layer as well as contact metallization in general, diffusion barriers are used in contact metallization, consisting either of layers of refractory metals or of interstitial phases that do not interact with surrounding metal and semiconductor layers [1].

In silicon electronics, contact layers are usually formed by silicides [2]. It turns out that depending on a variety of factors (such as surface processing, thermal treatment regimes, quality of initially evaporated metal layers, etc.), even at sufficiently optimal thermal treatment conditions (as it would seem at first sight), across the entire area of metal-Si interface, several silicide phases (previously well-known to researchers) are usually formed, each characterized by its own electron work function $\varphi_m$, [3], while, plethora of unknown silicide phases are shaped as well. This in turn implies that along the process, substantial metal-semiconductor interfacial inhomogeneity in terms of electrical properties appears that does not contribute to improving its reliability. In the present research paper, we investigate how ohmic contacts to *n+-Si* based on titanium silicide phases and *Ti*- and $TiB_x$-film diffusion barriers, are shaped.

**Techniques of measurement and samples**

The authors in the present investigation applied two types of samples, i.e., trial samples for measurement of $\rho_c$ by applying Transmission Line Method (TLM) as well as trial samples with metallization layers for measurement of distribution profiles of components by method of Auger spectroscopy in ohmic

contact before and after quick thermal treatment during 60 seconds at temperatures of 400 and 600 °C.

Single crystalline *Si* (111) doped with phosphorus ~$2 \cdot 10^{19}$ $cm^{-3}$, obtained by CZ technique was used as an initial sample. On preliminarily cleaned surface of *Si* that was heated to 150 °C, *Ti* (60 nm), $TiB_x$ (100 nm), *Ti* (60 nm) and *Au* (100 nm) layers were sequentially deposited by applying the technique of thermal evaporation of metals in vacuum. The first deposited layer of *Ti* was the contact-forming layer, the second one $TiB_x$ – is the diffusion barrier, and the following *Ti* layer is the diffusion barrier and adhesive layer at the same time that in turn ensures reliable contact of *Au*.

For measurement of $\rho_c$ we have used the previously mentioned reference method [4]. Distribution profiles of components in contact metallization layer were measured by applying Auger electron spectroscopy LAS-2000.

**Experimental and discussion**

The schematic diagram of *Au-Ti-*$TiB_2$*-Ti-n-Si* is shown on (Fig. 1). The $TiB_2$ – based diffusion barrier ensures high thermal stability of contact systems in the temperature range of 700 °C in QTT temperature mode. This takes place due to peculiarities of chemical bonds prevalent in $TiB_2$, characterized by high thermal stability, chemical inertia and melting temperature that is more characteristic of metals. Additional layer of *Ti* also serves as a diffusion barrier and ensures better adhesion of $TiB_2$ and *Au*.

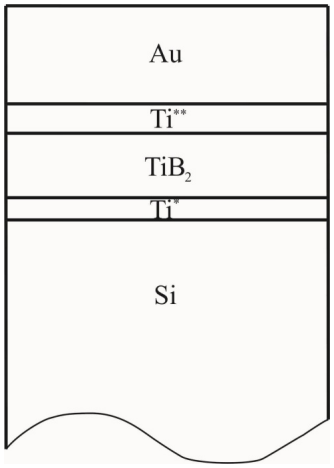


Figure 1. *Au-Ti-*$TiB_2$*-Ti-n-Si*-type *contact system structure*

*Si* – silicon sample doped with phosphorus;
*Ti** – contact-forming layer of titanium;
$TiB_2$ – diffusion barrier layer;
*Ti*** – additional diffusion barrier layer;
*Au* – outer contact layer of aurum

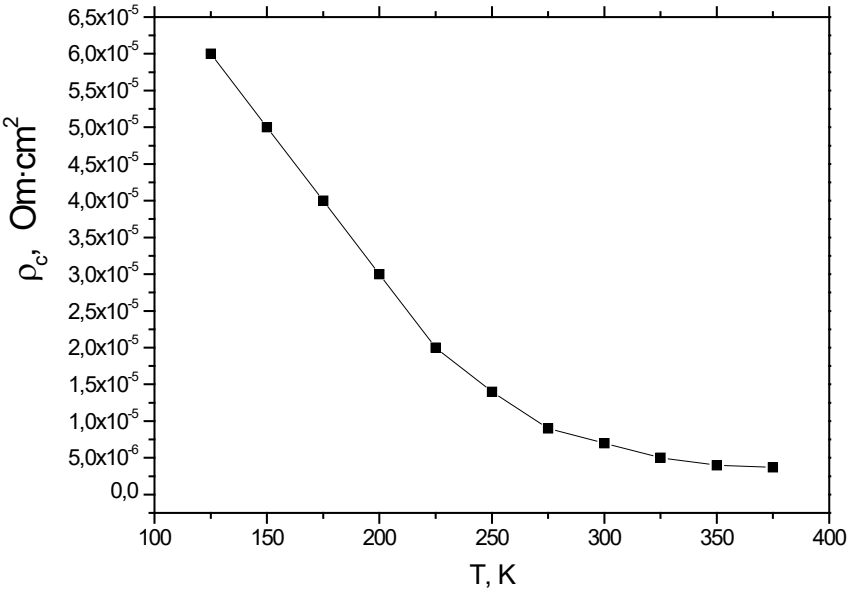


Figure 2. Temperature dependence of $\rho_c$ In *Au-Ti-*$TiB_x$*-Ti-*$n^+$*-Si*-type ohmic contact

The (Fig. 2) shows a temperature curve of dependence of $\rho_c$ of the initial sample (metals were applied on a sample surface heated up to 150 °C). As is shown in this figure in the measurement range from 125K to 375K, $\rho_c$ rather decreases. Such dependence of $\rho_c(T)$ manifests thermal field charge transfer behavior in ohmic contact [5].

As it is well known, majority of low power Si based microelectronics devices operate in the temperature range that does not exceed 100 °C. In this regard, we have measured the $\rho_c(T)$ dependence in the temperature range of 300–375 K before and after QTT.

The experimental results shown in (Fig. 3) reveal that the dependence of $\rho_c(T)$ before and after QTT at $T$ = 400 °C does not virtually change at all, whereas the behavior of $\rho_c(T)$ curve before and after QTT at $T$ = 600 °C in the measurement temperature range, had significantly increased.

The experiment reveals that the ohmic contact is formed along the process of deposition of metals on the surface of heated sample. The electron work function $\varphi_m$ for *Ti* is 3,95 *eV*, whereas for phases *TiSi*, $Ti_5Si_3$ and $TiSi_2$ it is 3,99 *eV*, 3,71 *eV* and 4,17 *eV*, respectively [3; 6]. These are data for the above phases that are shaped during the deposition process or QTT. These work functions are substantially lower in comparison with that of Si (4,8 *eV*) that allow forming ohmic contact even without having to carry out high temperature treatment.

Meanwhile, the existence in the contact-forming layer of comparatively low-temperature phases of *TiSi* и $Ti_5Si_3$ along with pure *Ti* characterized by slightly varying electron work functions allows forming relatively evenly distributed contact, evidenced by experiments (curves 1 and 2 on Fig. 3).

While the temperature of QTT increases to 600 °C, as the paper [7] reveals, an intensive formation of $TiSi_2$ phase takes place characterized with electron work function of ~ 4,18 *eV*, which in the existence of other silicide phases leads to shaping of unevenly distributed contact and an increase in the value of $\rho_c$ (curve 3 in Fig. 3).

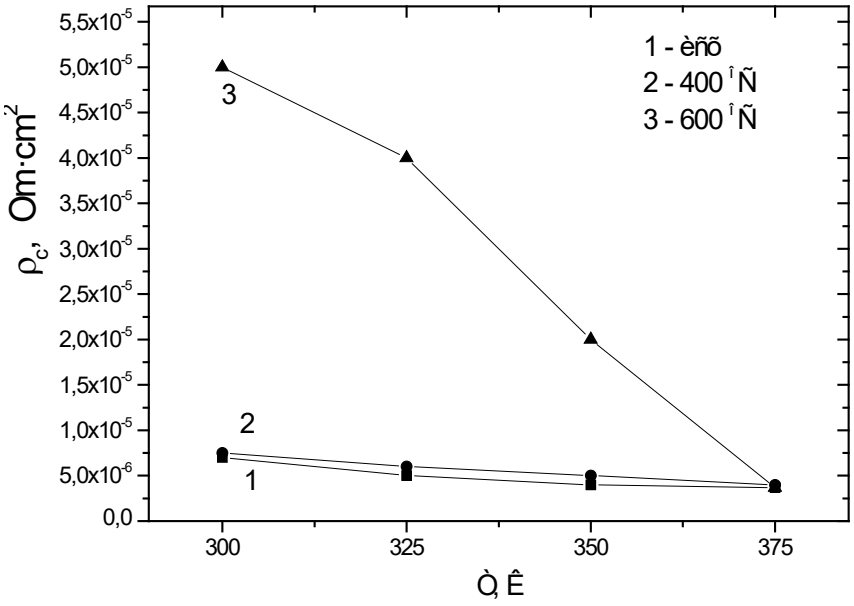


Figure 3. Dependence *of* $\rho_c$ on temperature before and after *QTT* at $T$ = 400 and 600 °C

The experimental dependence curves of $\rho_c(T)$ before and after QTT well correlate with distribution profiles of components in contact metallization layers (Fig. 4). As is evident from (Fig. 4 a, b), the results of profile distribution of initial sample and that of a sample that had undergone quick heat treatment at 400 °C

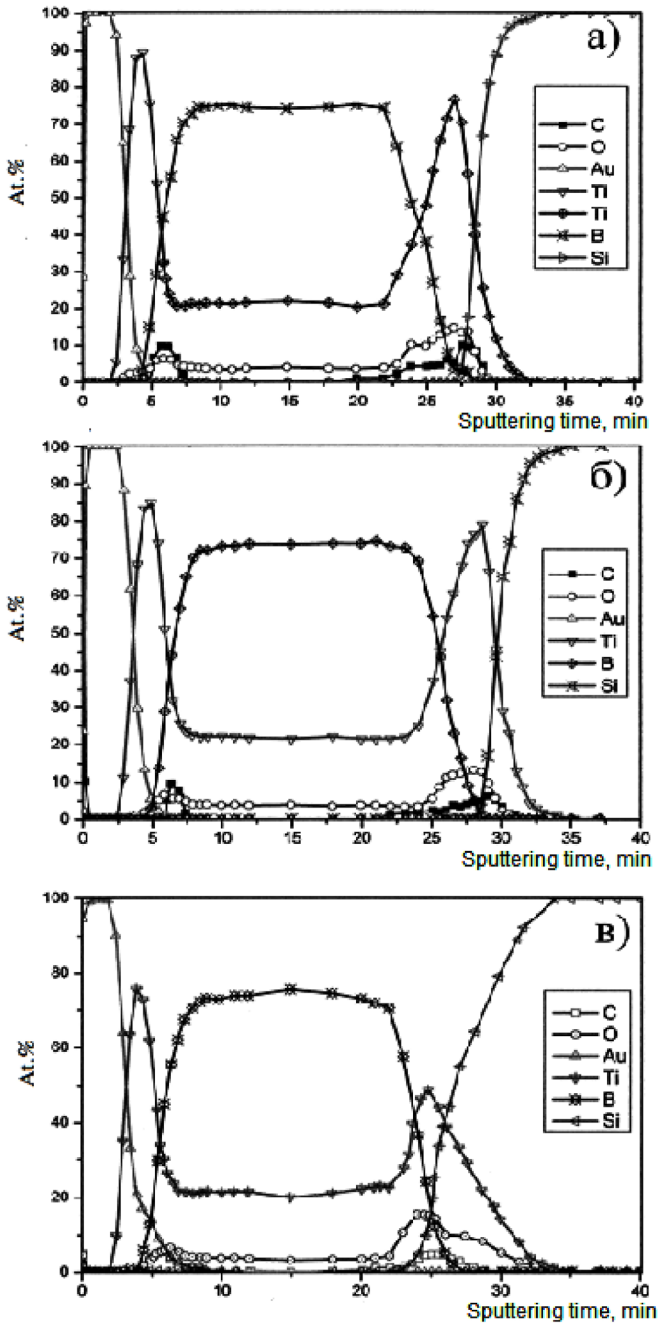


Figure 4. Profiles of distribution of components in *Au-Ti-TiB$_x$-Ti-n$^+$-Si* contact before (a) and after quick heat treatment at 400 °C (b) and 600 °C (c) during 60 seconds

are almost identical, whereas in the sample annealed at $T$ = 600 °C (Fig. 3, c) one can witness intensive mass transfer of Si towards contact shaping silicide layer.

This in turn, according to the data in [8] leads to shaping of $TiSi_2$ phase, thus in our case conditioning appearance of uneven contact and the increase in the value of specific contact resistance.

Judging by the profiles of distribution of components in *Au-Ti-TiB$_x$-Ti-n$^+$-Si* before and after QTT at 400–600 °C during 60 seconds, one can conclude that comparatively high quality of *Ti* and $TiB_x$ diffusion barriers precondition stability of interface *"contact forming layer – n$^+$-Si"* layers.

**Conclusion**

The experimental results indicate that a low-resistance *Au-Ti-TiB$_x$-Ti-n$^+$-Si* ohmic contact is formed in the course of deposition of metallization layer on a thermally heated (to 150 °C) n$^+$-Si substrate without having to additionally heat it afterwards in QTT regime. QTT at $T$ = 400 °C has practically no effect on distribution profile of the metallization layer components and the value of $\rho_c$ in comparison with the initial sample obtained by deposition of metals on a *Si* substrate heated to 150 °C. QTT at $T$ = 600 °C contributes to forming of $TiSi_2$ phase and, as a result, leads to occurrence of an inhomogeneous ohmic contact with a value of $\rho_c$ larger than $\rho_c$ of the initial sample and the one that had undergone heat treatment (QTT) at $T$ = 400 °C.

*Ti* and $TiB_x$ diffusion barriers manifest heat resistance after QTT at $T$=400 and 600 °C.

## References:

1. Агеев О. А., Беляев А. Е., Болтовец Н. С., Конакова Р. В., Миленин В. В., Пилипенко В. А. / Фазы внедрения в технологии полупроводниковых приборов и СБИС // – Харьков: НТК «Институт монокристаллов». 2008.– 385 с.
2. Мьюрарка Ш. / Силициды для СБИС // – М.: Мир. 1986.– 176 с.

3. Фоменко В. С. / Эмиссионные свойства материалов // Справочник.– Киев: Наукова думка. 1981.– 164 с.
4. Беляев А. Е., Болтовец Н. С., Капитанчук Л. М., Кладько В. П., Конакова Р. В., Кудрик Я. Я., Кучук А. В., Коростинская Т. В., Литвин О. С., Миленин В. В., Неволин П. В., Атаубаева А. Б. / Омические контакты Au-Ti-$n^+$Si, Au-Ti-$Pd_2$Si-$n^+$Si к кремниевым СВЧ диодам // Техника и приборы СВЧ – № 2. 2009.– С. 31–34.
5. Sze S. M., Kwok K. Ng. Physics of semiconductor devices. 3-rd edition, John Wiley & Sons, 2007. – 815 p.
6. Самсонов Г. В., Дворина Л. А., Рудь Б. М. / Силициды // Металлургия.– М. 1979.– 271 с.
7. Борисенко В. Е. / Твердофазные процессы в полупроводниках при импульсном нагреве // Под ред. В. А. Лабунова.– Минск: Навука и тэхника. 1992.– 248 с.
8. Dexin C. X., Harrison H. B., Reeves G. K. Titanium silicides formed by rapid thermal vacuum processing // J. Appl. Phys.– 63(3). 1988.– P. 2171–2173.

**https://doi.org/10.29013/AJT-22-9.10-31-35**

*Zikrillayev N. F.,*
*Faculty of Electronics and Automation*
*of Tashkent State Technical University,*
*Tashkent, Uzbekistan*

*Zikrillayev Kh.F.,*
*Faculty of Electronics and Automation*
*of Tashkent State Technical University,*
*Tashkent, Uzbekistan*

*Isakov B.,*
*Faculty of Electronics and Automation*
*of Tashkent State Technical University,*
*Tashkent, Uzbekistan*

*Qurbanov Sh.,*
*Faculty of Electronics and Automation*
*of Tashkent State Technical University,*
*Tashkent, Uzbekistan*

*Khaqqulov M.,*
*Joint Belarus-Uzbek Interbranch Institute*
*of Applied Technical Qualifications in Tashkent*

*Mahmudov S.,*
*Joint Belarus-Uzbek Interbranch Institute*
*of Applied Technical Qualifications in Tashkent*

# ON HOW TO CALCULATE THE BAND GAP OF SULFUR AND ZINC-DOPED SILICON

**Abstract.** The value of the band gap ($E_g$) is a core parameter of a semiconductor material. An exact knowledge of the band gap in such materials makes it possible to manipulate key performance characteristics of semiconductor devices developed on the basis of such materials [1]. Therefore, comprehensive knowledge of $E_g$ in a semiconductor material is one of the main issues of semiconductor physics and technology [2].

**Keywords:** semiconductor, new materials, value of the band gap, electronics, photoenergetics.

**Experimental technique**

The process of diffusion of impurity atoms of sulfur and zinc in silicon was carried out as follows. Initially, *n* – type conductivity phosphor-doped silicon samples with resistivity of $\rho$ =100 Ω cm (size $1 \times 5 \times \times 10\,mm^3$) were prepared as reference samples. These samples were divided into 2 groups and thereafter a two-stage process of diffusion of impurity atoms of sulfur and zinc in silicon was carried out from gaseous phase installation. At the first stage of diffusion, impurity atoms of sulfur were doped in silicon from gaseous phase in a vacuumed ($P \approx 10^{-6}$ mm. Hg)

quartz ampoules at temperature of $T$ = 1250 °C for $t$ = 10 hours. Reference samples in the second group, i.e., not doped with impurity atoms of sulfur and zinc were put into in a separate quartz ampoule and subjected to annealing under similar thermal and technological conditions. At the second stage, silicon samples from both groups were placed in quartz ampoules and diffused with impurity atoms of zinc. Diffusion of zinc atoms was carried out in separate quartz ampoules under the same conditions at a temperature of $T$ = 1200 °C for $t$ = 5 minutes.

After diffusion, the surfaces of silicon samples were cleaned by mechanical and chemical treatment. Diffusion of impurity atoms of sulfur and zinc in silicon allowed us to receive structures with a $\rho$ –$n$ junction. After the diffusion process has been accomplished, 100 $\mu$m-thick samples were polished (i.e., surface layers) by mechanical grinding from five sides (with the exception of one side). (Figure 1 a, b).

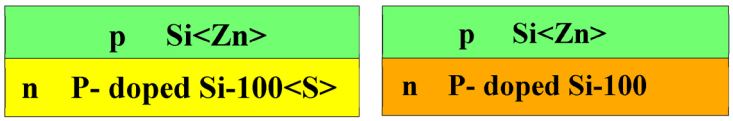


a) b)

Figure 1. Structure of $\rho$ –$n$ junction, formed on the basis of $n$ – type conductivity phosphor-doped silicon samples with resistivity of $\rho$ = 100% cm *a) samples of the 1st group, b) samples of the 2nd group*

In the process of grinding, in order to determine the depth of diffusion of impurity atoms in silicon samples, the type of conductivity of $\rho$ – $n$ junctions on the surface of the samples were assessed using a two-probe technique (thermal probe). The depth of of zinc and sulfur impurity atoms in silicon was calculated using theoretical formulas taking into account the diffusion mechanism of sulfur and zinc impurity atoms in silicon. The calculated depth of impurity atoms in silicon samples and the actual depth determined after the diffusion process were in good concordance only with negligent difference of ~5% [3–5].

At various temperatures, the authors measured the current-voltage characteristics (CVC) of the samples where $\rho$ – $n$ junction were formed. Their spectral sensitivity was also measured at room temperature by using IKS-12 spectrophotometer in the visible light range.

**Measurement technique**

For measuring the current-voltage characteristics (CVC), a device was used that was designed as per (Fig. 2). Current-voltage characteristics of *Si* < *P*, *Zn* > and *Si* < *P*, *S*, *Zn* > samples with $\rho$ – $n$ junction were measured at two temperatures: $T_1$ = 30 °C and $T_2$ = 80 °C.

The current-voltage characteristics of the samples were measured using a DC source with a voltage of $U$ = 5$V$ and $U$ = 12$V$, a multi-stage potentiometer with a resistance of 10 kOhm, while current measurements were carried out using a Rigol DM3068-type device, voltage measurements were carried out with a Mastech MS8040 device, a thermostat connected to a constant voltage source, digital temperature meter type Espada TPM10 with scale division of $\Delta t$ = 0.1 °C. In order to prevent significant overheating of $\rho$ – $n$ structures, the measurements were carried out by applying short-term impulse voltages. The results of the current-voltage characteristics of samples with a $\rho$ – $n$ junction are shown in (Fig. 3).

The authors in [1] based on I–V characteristics of $\rho$ – $n$ structures suggested the final formula for determining the band gap ($E_g$) of a semiconductor material with a $\rho$ – $n$ junction:

$$E_g = \frac{T_1 T_2}{T_2 - T_1}\left[\left(\frac{\varphi_{c1}}{T_1} - \frac{\varphi_{c2}}{T_2}\right) - 3k\ln\frac{T_2}{T_1}\right] \qquad (1)$$

where: $T_1$ and $T_2$ are experimental temperatures; $\varphi_{c1} = U^c_{cut1}$ and $\varphi_{c2} = U^c_{cut2}$; is the Boltzmann constant; $E_g$ is the band gap energy of a semiconductor material.

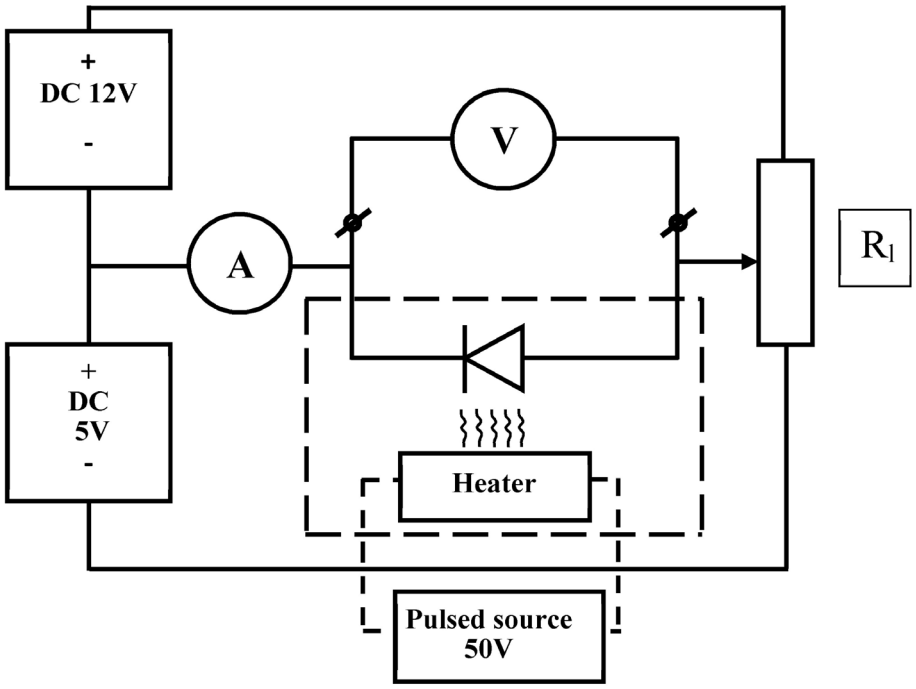


Figure 2. The device for measurement of current-voltage characteristics of the samples

Afterwards, straight lines were drawn from the linear parts of the current-voltage characteristics of the samples at temperatures $T_1$ = 30 °C and $T_2$ = 80 °C, and from the points of their intersection with the voltage axis, the values $U_{cut1}^{C}$ and $U_{cut2}^{C}$ were determined. As a result of measurement of I–V characteristics of the samples and by applying formula 1, the value of the energy of the band gap, was determined [6].

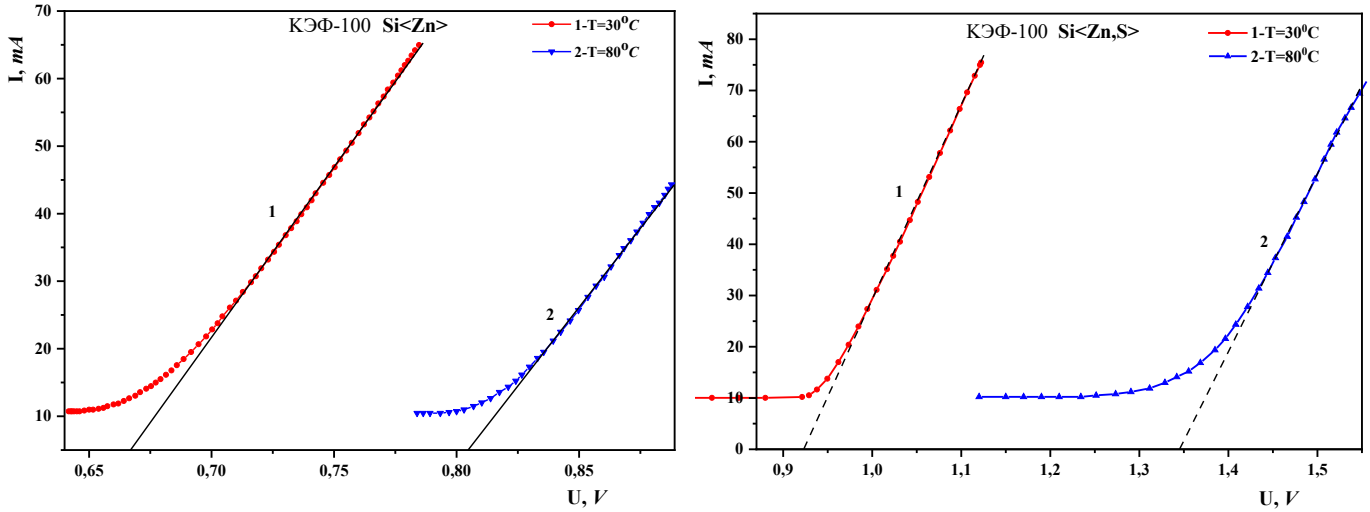


a) b)

Figure 3. Current-voltage characteristics (CVC) of silicon samples containing impurity atoms of zinc and sulfur, measured at temperatures: $T$ = 30 °C and 2– $T$ = 80 C: a) Zn-doped silicon (initial sample of n-type conductivity phosphor-doped silicon with resistivity of $\rho = 100\,\Omega$ cm); b) *Zn* and *S* doped silicon (initial sample of *n* – type conductivity phosphor-doped silicon with resistivity of $\rho = 100\,\Omega$ cm)

As a result of measurements and the data presented in (Fig. 3) and further by applying formula 1, the band gap energies were determined: $Eg_{Si_{Zn}} \approx 1.14\,eV$ – for silicon samples containing zinc

atoms and $Eg_{Si_{Zn}} \approx 1.38 eV$ – for silicon samples containing binary compounds of impurity atoms of sulfur and zinc.

It is well known that the fundamental value of the band gap of a single crystalline silicon equals $Eg \approx 1.12\ eV$, whereas the value of the band gap of a pure single-crystalline zinc-sulfide semiconductor compound is $Eg \approx 3.72\ eV$. The value of the band gap energy of the formed $ZnS$ binary compound in silicon, determined experimentally, looks likely to be $Eg_{Si<Zn>S} = 1.38\ eV$, which is also confirmed by theoretical calculations $\left(Eg_{Si} < Eg_{Si<ZnS>} > Eg_{ZnS}\right)$ using formula 1.

Based on the analysis of the experiments, the authors suggest that new sulfide-zinc binary compounds type $(ZnS)_x(Si_2)_{1-x}$ must be formed in the bulk of single-crystalline silicon. In the course of investigation at room temperature of spectral sensitivity of the obtained silicon samples with impurity atoms of zinc as well as of silicon samples sequentially doped with impurity atoms of sulfur and zinc, it was determined that in silicon samples containing impurity atoms of sulfur and zinc one might evidence the increase in the sensitivity and expansion of the spectral range towards visible diapason [7–9].

As can be seen from (Fig. 4), the maximum photocurrent density of silicon samples containing sulfur and zinc atoms (second curve) is almost 3 times higher than the maximum photocurrent density of silicon samples containing only zinc atoms (first curve). In addition, the expansion of the range of absorption of light rays from $\Delta E_1 = 0.4\ eV$ to $\Delta E_2 = 0.93$ eV is well evidenced.

The experimental results suggest that by embedding sulfur and zinc atoms into the lattice of single-crystal silicon, one might form binary neutral compounds of $Zn - S^{++}$ type. It has been established that these binary compounds formed in the volume of silicon lead to a change in the fundamental parameters of silicon, which makes it possible to obtain a material with absolutely novel electrophysical parameters.

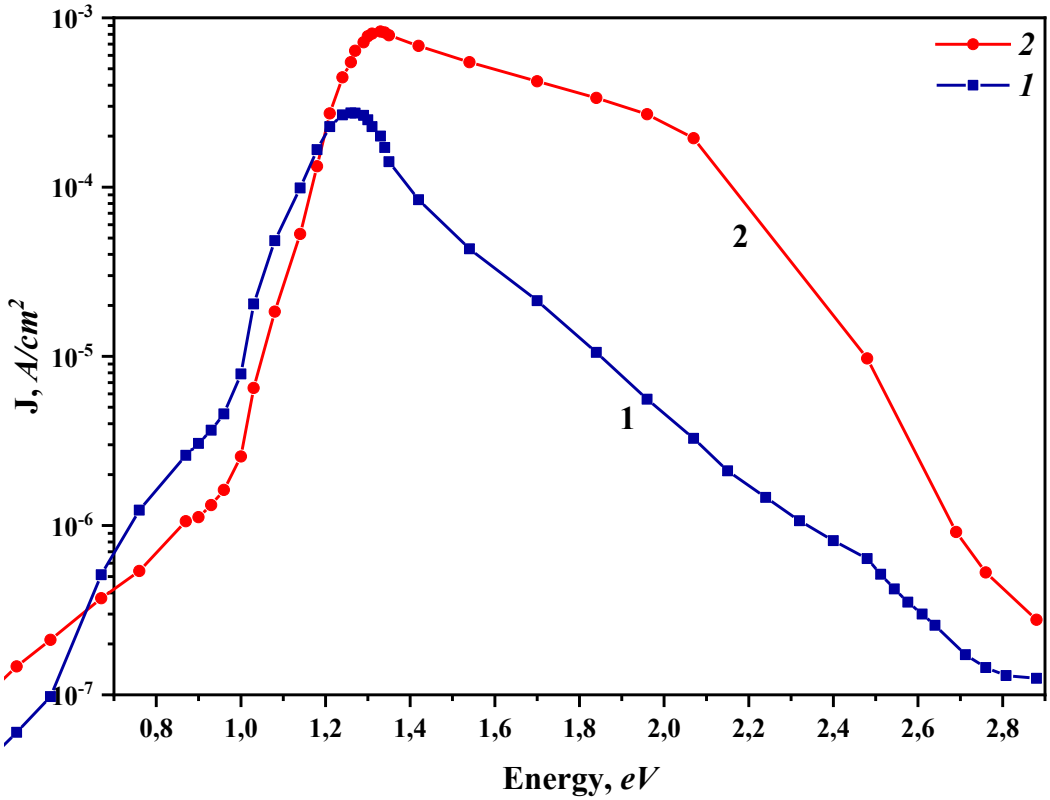


Figure 4. Spectral characteristics of samples: 1 – *Si < P, Zn >*; 2 – *Si < P, S, Zn >*, $T = 300\ K$, $U = 10\ V$

The parameters of such a material fundamentally differ from the fundamental parameters of silicon. As a result of X-ray diffraction studies, it was established that the formed binary compounds of sulfur and zinc do not affect the crystal structure of the initial silicon [10–12].

**Conclusion**

Thus, the authors report that a technology has been developed that would allow obtaining new materials with impurity atoms of sulfur and zinc in silicon, which leads to the formation of binary compounds from sulfur and zinc atoms, thus changing the fundamental parameters of the source material. It is shown that the obtained silicon samples containing binary compounds of impurity atoms of sulfur and zinc could help to design cheap devices for their implementation in electronics, optoelectronics, and photoenergetics.

**References:**


1. Викулин И. М., Коробицын Б. В., Криськив С. К. Методы определения ширины запрещенной зоны полупроводниковых структур с p-n-переходами. Физика и техника полупроводников,– Том 50.– Вып. 9. 2016.– С. 1238–1241.
2. Mc Cloy John and Tustison Randal. Chemical vapor deposited zinc sulfide, Published by SPIE The International Society for Optical Engineering P. O. Box 10 Bellingham, Washington USA, 2013.– P. 1–9.
3. Бахадырханов М. К., Исамов С. Б., Зикриллаев Н. Ф. Особенности вольт-амперной характеристики кремния с нанокластерами атомов марганца. Неорганические материалы,– Том 50.– № 4. 2014.– С. 353–357.
4. Razykov T. M., Patryn A., Malinski M., Bychto L., Ergashev B., Kouchkarov K., Shukurov A., Makhmudov M., Isakov D. Optical Properties of CdS1 – xTex Thin Films Obtained by Chemical Molecular Beam Deposition Method (2021) Applied Solar Energy (English translation of Geliotekhnika),– 57 (3).– P. 181–187.
5. Ганина Н. В. Физико-химические особенности изовалентного легирования полупроводников. Physics and Chemistry of Solid State.– V. 3.– № 4. 2002.– P. 565–572.
6. Joongoo Kang, Ji-Sang Park, Pauls Stradins, and Su-Huai Wei. Nonisovalent Si-III–V and Si-II–VI alloys: Covalent, ionic, and mixed phases. Physical Review – – Vol. 96.– Issue 4. 2017 B.– 045203.
7. Baxadyrhanov M. K., Sodikov U., Zikrillaev N. F., Norkulov N. Razrabotka fizicheskih osnov nanorazmernyh struktur na osnove molekuloobrazovaniya S++Mn- – i Se++Mn- – v reshetke Si. Elektronnaya obrabotka materialov,– No. 5. 2007.– P. 106–108.
8. Бондарь И. В. ФТП,– 49 (3). 2015.– 1180 с.
9. Лебедев А. И. Физика полупроводниковых приборов.– М., Физматлит, 2008.
10. Питер Ю., Кардона М. Основы физики полупроводников.– М., Физматлит, 2002.
11. Гаман В. И. Физика полупроводниковых приборов.– Томск, Изд-во НТЛ, 2000.
12. Абдурахманов Р., Мавлянов А. Ш., Содиков У. Х., Норкулов Н. Новые материалы для солнечных элементов на основе кремния с квантовыми ямами CdS и Zn S. Электронная обработка материалов.– № 4. 2005.– С. 89–92.

# Section 5. Chemistry

https://doi.org/10.29013/AJT-22-9.10-36-40

*Alieva Mukaddas Tuychievna,*
*Candidate of chemical sciences, associate professor,*
*Tashkent State Technical University, Uzbekistan*
*Ikhtiyarova Gulnora Akmalovna,*
*Doctor of Chemical Sciences, Professor,*
*Tashkent State Technical University, Uzbekistan*
*Kholturayeva Noroy Ruzmatovna,*
*Candidate of chemical sciences, associate professor,*
*Tashkent State Technical University, Uzbekistan*

## OBTAINING COMPOSITIONS BASED ON LOCAL RAW MATERIALS FOR TEXTILE INDUSTRIAL WASTEWATER TREATMENT

**Abstract.** In this article, the organosorbent was obtained by modifying the bentonites of Navbakhor, a deposit on the territory of the Republic of Uzbekistan, in the presence of chitosan. The physicochemical properties of organosorbents were studied using modern spectrophotometric methods: a UV-5100 spectrophotometer and an Eye One Pro reflectance spectrum minispectrophotometer. The methods of waste water treatment of textile industries from ions of various metals, dissolved salts and residues of pigment dyes were studied, the determination of macro- and microelements by inductively coupled plasma mass spectrometry (ICP-MS) was studied.

**Keywords:** Waste water, chitin, chitosan, bentonite, modification, macro- and microelements by inductively coupled plasma mass spectrometry (ICP-MS).

**Introduction**

In recent years, a large amount of waste water has accumulated in industrial enterprises around the world. Cleaning them and returning them to the system is one of the urgent problems. However, cleaning them is a multi-step process that takes a lot of time. Treatment of industrial wastewater should be carried out taking into account their composition. Waste treatment methods are divided into: mechanical, chemical, physico-chemical and biological types, but when they are used together, the method of wastewater treatment and disposal is called a combined method [1–5].

**The main part**

The use of this method is determined in each specific case by the nature of pollution and the harmful level of released compounds. One of the methods of chemical cleaning of waste, especially of the textile industry, is cleaning with the help of various adsorbents. In this work, the organosorbent obtained as a result of modification named of Navbahor bentonite of the Republic of Uzbekistan with chitosan

was used. Industrial wastewater of textile enterprises was taken as an object. When their composition was studied, it was found that they consist of various metal ions, dissolved salts and pigment dye residues.

Chitosan is basically derivative form after the process of modification of chitin. It is a high molecular polymer glucosamine, it is soluble in a mixture of organic and inorganic acids. However, chitin is insoluble, while chitosan is soluble in acidic solutions. It can be used in various fields, agriculture and medicine. One of the obvious problems in the chitosan extraction process is the regeneration or sterilization of the highly effective alkaline solution in the wastewater. In most cases of the reaction process, the alkali concentration is reduced by 30–50% alkali solution. It is not allowed to place the reagent directly into the sewer. It is widely used for the dyeing of occasionally active and pigmented cotton materials, as well as for the dyeing of protein and cellulose mixed fabrics with acid-active dyes [6–7]. Compositions obtained on the basis of modification of bentonites with chitosan are used in agriculture, textile, medical and wastewater treatment, paper industry quality level, cosmetics, food production, veterinary and also. various industries for practical purposes.

**Determination of macro- and microelements by inductively coupled plasma mass spectrometry (ICP-MS).** This method was used to determine the elements of calcium, phosphorus, magnesium, iron and iodine in food products. for this, 0.0500––0.500 g of the test substance is measured on an analytical balance and placed in a Teflon container of an autoclave, then an appropriate amount of purified concentrated mineral acids (nitric acid and hydrogen peroxide) is added to it. The autoclave is closed and placed in a Berghof program controlled microwave digester (MWS-3+). Depending on the type of test substance, the appropriate program is determined. After decomposition of the substances placed in the autoclave, they are placed in volumetric flasks with a capacity of 50 or 100 ml and brought to the required mark with 0.5% nitric acid. Substances were detected using an ISPMS or a similar emission spectrometer with an inductively coupled argon plasma. The following equipment was used for the above analysis. ISPMS NEXION-2000 or similar mass spectrometer, microwave separators (Germany) or similar Teflon autoclave: flasks of various sizes. Reagents used: Multi-element standard #3 (29 elements for MS) Standards – mercury, nitric acid, hydrogen peroxide, bidistilled water and argon (gas purity 99.995%) [8].

**How to use Eye One Pro.** To carry out measurements, the Eye One Pro mini spectrophotometer was connected to the USB port of a computer, the Eye One Share program installed on the computer was launched in Windows, and the device was calibrated using a white substrate included in the standard set [30]. After that, the samples were measured, and the resulting data was exported to Excel as a series of reflection coefficients for different wavelengths. For each diffuse reflectance spectrum acquired with the Eye One Pro, the Kubelka-Munky F-function F was calculated and the diffuse reflectance intensity was observed to be related as follows:

$$F(R) = (1 - R)2/2R = 2.3c\varepsilon/S,$$

Here $R$ – is the diffuse reflection coefficient; $\varepsilon$ – molar absorption coefficient of the sorbate, $M$-1 $cm^{-1}$; c is its concentration, $M$; $S$ – scattering coefficient, $cm^{-1}$ [9–10].

**Discussion of the results.** Indigo dye solutions of different concentrations were prepared for this purpose. The absorbance level of indigo dye was determined on a UV-5100 spectrophotometer at a wavelength of 315 nm. The obtained results are presented in the following table 1 and (figure 1).

The results of the obtained analysis show that the amount of adsorption absorption of indigo dye in the prepared solution with a concentration of 1–– 30 mg/l decreases from 96.1% to 34.84%, that is, its absorption capacity can be seen to decrease as the concentration increases. The concentration of indigo dye in 20 and 30 mg/l solutions is almost close, indicating that it has reached its saturation point.

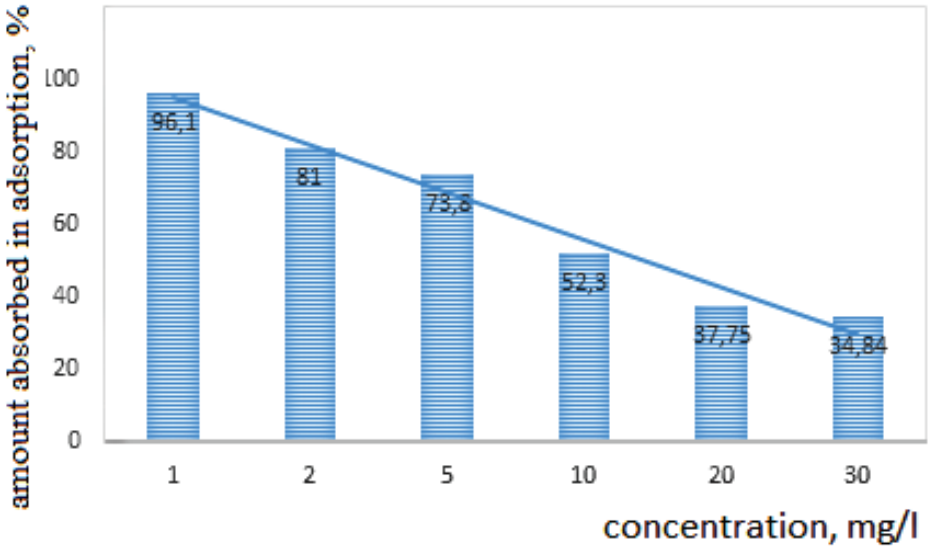


Figure 1. Dependence of indigo dye solution adsorption on solution concentration

Table 1.– Dependence of indigo dye adsorption on solution concentration

| Indigo dye, concentration, mg/l | Amount absorbed in adsorption mg/l | Amount remaining in solution after adsorption, mg/l | The absorption concentration of the solution,% |
|---|---|---|---|
| 1 | 0.961 | 0.039 | 96.1 |
| 2 | 1.62 | 0.38 | 81.0 |
| 5 | 3.69 | 1.31 | 73.8 |
| 10 | 5.23 | 4.77 | 52.3 |
| 20 | 7.55 | 12.45 | 37.75 |
| 30 | 10.45 | 19.55 | 34.84 |

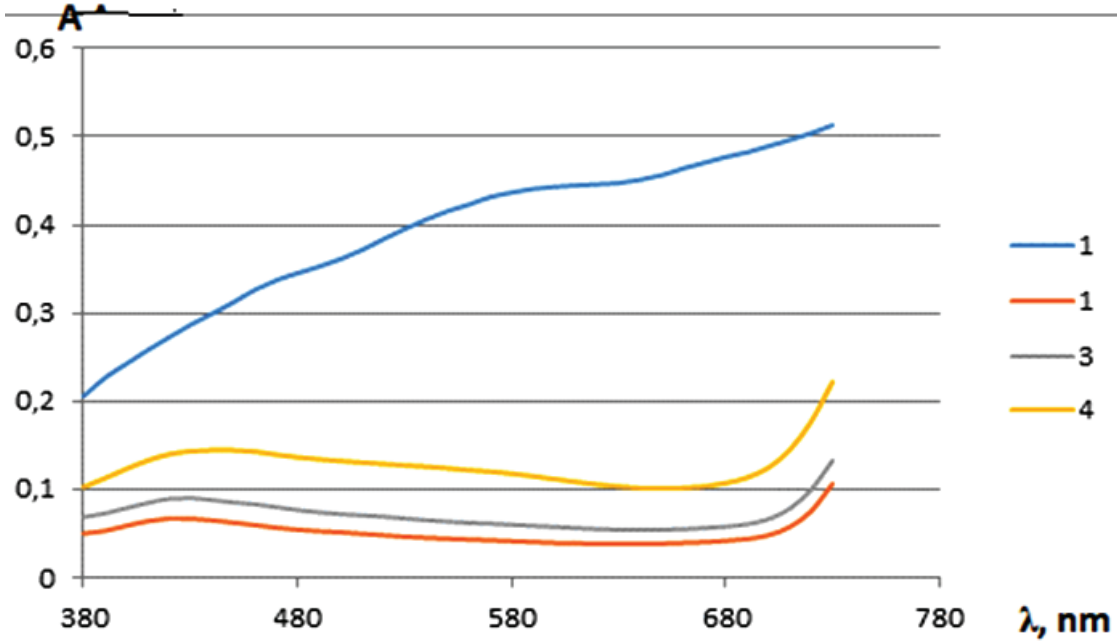


Figure 2. Navbakhor alkaline bentonite PBMB (1), Bentonite modified with chitosan (2), Water (3), Waste water (4) reflection spectrum

The reflection spectra of the obtained sorbents were studied.

As can be seen from (Figure 2), it is known in the absorption spectra of organosorbents that the maximum of the analytical signal is observed at 310 nm for textile wastewater, and after absorption on the organosorbent it is found that it has a maximum of the analytical signal at 540–550 nm.

As a result of the analysis of the absorption spectra of organosorbents, a bathochromic shift of the absorption maximum was observed, which can be explained by the absorption of various metal ions, dissolved salts, and pigment dye residues in wastewater. In addition, it undergoes various dissociation processes in various media.

In order to determine the degree of purification of wastewater from textile industries from various metal ions, dissolved salts and residues of pigment dyes, a study of macro- and microelements was carried out by inductively coupled plasma mass spectrometry (ICP-MS) [11–12].

Table 2.– Results of ICP-MS analysis of the amount of heavy elements

| samples | Ti mg/l | V mg/l | Cr mg/l | Mn mg/l | Co mg/l | Zr mg/l | Mo mg/l | Ag mg/l | Ba mg/l | Pb mg/l |
|---|---|---|---|---|---|---|---|---|---|---|
| Waste water | 0.080 | 0.066 | 0.208 | 0.204 | 0.007 | 0.016 | 0.029 | 0.008 | 0.263 | 0.019 |
| Waste water treatment with modified bentonite | 0.064 | 0.056 | 0.155 | 0.147 | 0.004 | 0.010 | 0.012 | 0.001 | 0.133 | 0.015 |

The analysis of heavy metals in wastewater samples brought from Delta Rumino Limited Liability Company located in the Republic of Uzbekistan and wastewater samples treated with bentonite modified with Apis mellifera chitosan was determined using plasma inductively coupled mass spectrometry (PIB-MS) (table 2).

As can be seen from the above table, we observed a decrease in the amount of heavy metals: titanium, vanadium chromium, manganese, cobalt, gallium, molybdenum, silver, barium, lead in the sample of wastewater brought from "Delta Rumino" LLC.

**Conclusion and recommendations:** In short, it indicates the possibility of using colored dyes from the composition of textile industrial wastewater in the sorption of our organosorbents. The results obtained are characterized by high selectivity, accuracy and expressiveness.

In conclusion, wastewater treatment of heavy metal ions by sorption method is one of the most suitable methods for industrial enterprises. At the same time, the water is softened, which makes it possible to use water in the circulating water supply.

## References:

1. Марченко Л. А. Исследование возможности сорбционной очистки при ликвидации нефтяных загрязнений / Л. А. Марченко, Е. А. Белоголов, А. А. Марченко, О. Н. Бугаец, Т. Н. Боковикова // Научны й журнал Куб ГАУ. – №84 (10). 2012. – С. 23–32.
2. Хальченко И. Г., Шапкин Н. П., Свистунова И. В., Токарь Э. А. Химическая модификация вермикулита и исследование его физико-химических свойств "Международном научном форуме Бутлеровское наследие 2015". URL: http://foundation.butlerov.com/bh-2015
3. Ихтиярова Г. А., Умаров Б. Н., Исомитдинова Д. С. Туробджанов С. М. Очистка сточных вод текстильного предприятия композиций на основе вермикулита и модифицированного хитозана. Журнал Композиционные материалы. – №4. 2021. – С. 116–118.
4. Ikhtiyarova G. A., Umarov B. N., Turabdjanov S. M. Purification of textile wastewater by vermiculite modified with chitosan // International Journal of innovative research. – Vol. 9. – Issue 9. 2021. – С. 9780–9786.

5. Алиева М. Т., Ихтиярова Г. А., Умаров Б. Н. Модификация вермикулита и бентонитовой глины с хитозаном и исследование адсорбционных свойств органосорбентов для обезвреживания сточных вод. Международная научно-практическая конференция «Интеграция науки, образования и производства – залог прогресса и процветания». – Т. II. – г. Навои, РУз, 2022. – С. 24–26.
6. Ikhtiyarova G. A., Umarov B. N., Turabdjanov S. M., Mengliyev A. S., Usmanova G. A., Axmadjonov A. N., Haydarova Ch. Q. Physicochemical properties of chitin and chitosan from died honey bees Apis Mellifera of Uzbekistan. Journal of Critical Reviews. – Vol 7. – Issue 4. 2020. – P. 120–124.
7. Ixtiyarova G. A., Hazratova D. A., Umarov B. N., Seytnazarova O. M. Extraction of chitozan from died honey bee apismellifera // International scientific and technical journal Chemical technology control and management. – Vol. 2020. – ISSN. 2. – Article 3. – P. 15–20.
8. Саввин С. Б., Штыков С. Н., Михайлова В. В. Органические реагенты в спектрофотометрических методах анализа // Успехи химии. – Т. 75. – №4. 2006. – 380 с.
9. Jankiewicz B. Spectrophotometric Determination of Iron (II) in the Soil of Selected Allotment Gardensin Łódź / B. Jankiewicz, B. Ptaszyński, A. Turek // Polish Journal of Environmental Studies. – V. 11. – No. 6. 2002. – P. 745–749.
10. Иванов В. М., Фигуровская В. Н. Цветометрические характеристики тиоцианата железа (III) // Вестн. – Моск. ун-та. Сер. 2. Химия. – Т. 45. – № 5. 2004. – 315 с.
11. Akao M., Yamazaki A., Fukuda Y. Vermiculite board for novel building material. J. Mater Sci Lett – 22(21). 2003. – P. 1483–1485.
12. Karatas M., Benli A., & Toprak H. A. Effect of incorporation of raw vermiculite as partial sand replacement on the properties of selfcompacting mortars at elevated temperature. Construction and Building Materials, – 221. 2019. – P. 163–176.

**https://doi.org/10.29013/AJT-22-9.10-41-45**

*Rahmanberdiev Gappar,*
*professor, Tashkent chemical-technological Institute*
*Khusenov Arslonnazar,*
*professor, Tashkent chemical-technological Institute*
*Ibragimova Komila,*
*researcher, Tashkent Chemical – Technological Institute*
*Tilakov J. R.,*
*researcher, Tashkent Chemical – Technological Institute*
*Baltabaev Ulugbek Narbaevich,*
*associate, Tashkent chemical-technological Institute*

# ANALYSIS OF INULIN OBTAINED FROM THE POWDER OF TOPINAMBOUR TUBERS (HELIANTHUS TUBEROSUS L.)

**Abstract.** Obtaining possibility of inulin from powders from topinambour tubers has been shown. Qualitative and quantitative analyses of the obtained product have been resulted. Results of researches have been showed that purified inulin contains more than 86% pure inulin.

**Keywords:** topinambour tubers, inulin, dissolves, spectrum, characteristic, fructose, glucose.

**Introduction**

Now in process of active studying of properties of topinambour in many countries of the world (Japan, the USA, Canada, Holland, Belgium, Germany, etc.) physicians manifest huge interest to it as to medical and dietary means. 100% of the concentrate of topinambour tubers contains high concentration of inulin. Inulin represents difficult carbohydrates, in many respects similar on structure with starch and cellulose, but it consists of fructose by 95%.

The purpose of our work is qualitative and quantitative analysis of inulin obtained the powder of topinambour tubers (Helianthus tuberosus L.) which has the following chemical formula:

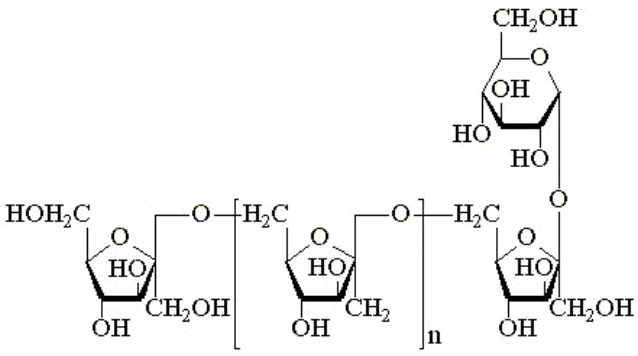

The basic technological circuit design of obtaining inulin includes purification stages (peeling), cutting, drying, crushing, screening, dissolution, sedimentation, drying of a deposit, crushing, screening and packing [1].

At obtaining powder of topinambour tubers it is pleaded with a knife or the special apparatus. For this purpose at first the crude is washed out from mechanical pollution, then it is peeled, the purified raw materials are subjected to cutting and dried at

temperature 55–65 °C in a current of hot air or under vacuum at 1–5 mm of mercury column. The obtained product is subjected to crushing within 80 minutes in the ball mill, sieved through a sieve (C-10) with diameter of apertures 0,1 mm. The powder has from white to dark-cream colour with dark impregnations. Specific odor. Taste, as raw materials. pH of 0,1%-s' aqueous solutions has been defined by potentiometer method and equated 7–7.5 [2; 3].

The quantity of inulin has been defined on the solubility in water, in ethyl spirit and on optical density.

Polysacharide inulin (fructosane) dissolves in hot water well and does not dissolve in ethyl alcohol. Fructose and low-molecular fructoside dissolve both in water, and in ethyl alcohol. On the difference between fructoside and fructosane the quantity of inulin has been computed.

The amount of fructoside and fructosane has been defined on the method [4] in the following way.

About 1 g of raw materials was placed in a conic flask capacity of 200 ml, 60 ml of water was added and heated up on the boiling water bath with the reflux condenser within 45 minutes. Warm extraction was filtrated through cotton wool in a measured flask capacity of 200 ml so that raw materials corpuscles did not get on the filter. The flask was rinsed with 10 ml of water and filtrated in the same measured flask. Extraction was repeated by two more times (the first time 45 minutes with 30 ml of water heated up, second – 15 minutes with 30 ml of water). Both extraction were filtrated in the same measured flask and washed out the rest on the filter, using each time by 10 ml of water. Cotton wool with raw materials was squeezed.

2 ml of 10% of a solution of acetate of basic lead was added in to the obtained mixture, mixed and left for 10 minutes. Then 2 ml 5%-s' solution of phosphate sodium was added, mixed and left for 5 minutes. The volume of solution in the flask was led up to mark with water and mixed. Extraction was filtrated through the paper folded filter, the first 10–15 ml of filtrate was discarded. 2 ml of filtrate was placed in a measured flask capacity of 100 ml, the volume of solution was led up to mark with water and mixed (solution A).

5 ml of 0.1% alcohol solution of resorcin was placed into the measured flask capacity of 25 ml. Then 5 ml of the solution A (an analyzed solution) was added into the flask. The volume of solution was led up to mark of 30% with the solution of hydrochloric acid, then it was mixed. Flask contents were poured into a test tube and heated up on the water bath at temperature 80 °C during 20 min., then it was cooled at room temperature.

Optical density of the solution under test was measured by the spectrophotometer ("Genesis" of the USA wave length 190–1100 nanometers) at wave length of 482 ± 2 nanometers in a cuvette with thickness of a layer of 10 mm concerning a comparison solution.

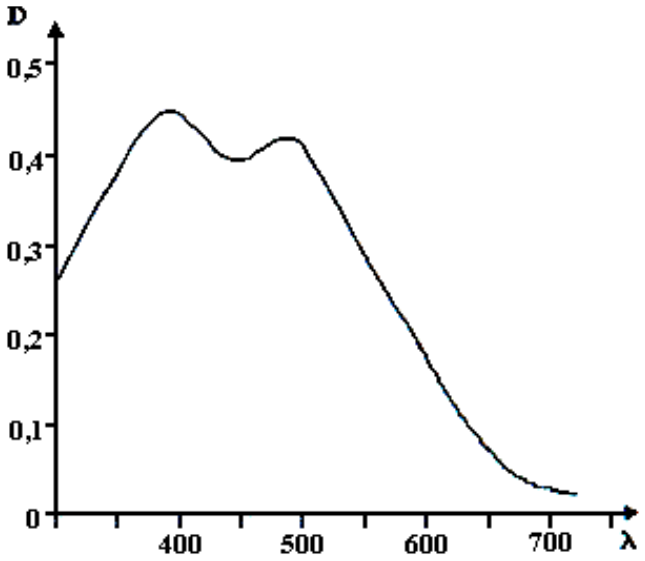


Figure 1. Absorption spectrum of reaction product of interaction of fructose with resorcin in the acid medium

The total content of fructosides and fructosanes in conversion on fructose and absolutely dry raw materials in percentage (X) was computed by the formula:

$$X = \frac{D \cdot 200 \cdot 100 \cdot 100}{95 \cdot 1 \cdot 2 \cdot m \cdot (100 - W)} = \frac{0.824 \cdot 200 \cdot 100 \cdot 100}{95 \cdot 1 \cdot 2 \cdot 1 \cdot (100 - 3)} = 89.4195\%, \quad (1)$$

where D – optical density of an analyzed solution; 95 – a specific absorption coefficient of a reaction product of interaction of fructose with resorcin in acid medium; m – weight of raw materials in gr; W – loss in weight at raw materials drying in%.

The quantity of fructosides was defined by the technique [4] as follows: about 1g raw materials was placed in a conic flask capacity of 200 ml, 60 ml of 95% of alcohol was added and heated up on the boiling water bath with the reflux condenser within 45 minutes. Warm extraction was filtrated through a cotton wool layer in a measured flask capacity of 200 ml so that raw materials corpuscles did not caught on the filter. The flask was rinsed with 10 ml of 95% alcohol and filtrated in the same measured flask. Extraction was repeated by two more times, (the first time heated up within 45 minutes about 30 ml of 95% alcohol, the second time – 15 minutes about 30 ml of 95% alcohol). Raw materials were transferred on the filter, the flask was rinsed, and then the residue was washed out on the filter, using each time on 10 ml of 95% alcohol. Cotton wool with raw materials was squeezed.

1ml of 10% of a solution of acetate of basic lead was added in to the obtained mixture, mixed and left for 10 minutes. Then 2 ml of 5%-s' solution of phosphate sodium was added, mixed and left for 5 minutes. The volume of solution in the flask was led up to mark with water and mixed. Extraction was filtrated through the paper folded filter, the first 10–15 ml of filtrate was discarded. 10 ml of filtrate was placed in a measured flask capacity of 100 ml; the volume of solution was led up to mark with water and mixed (solution A).

5 ml of 0.1% alcohol solution of resorcin was placed into the measured flask capacity of 25 ml. Then 5 ml of the solution A (an analyzed solution) was added into the flask. The volume of the solution was led up to mark with 30% of hydrochloric acid solution, and it was mixed. Flask contents were poured in a test tube and heated up on the water bath at temperature 80 °C during 20 min., and cooled at room temperature.

Optical density of the solution under test was measured by the spectrophotometer at wave length of 482 ± 2 nanometers in a cuvette with thickness of a layer of 10 mm concerning a comparison solution.

Preparation of a solution of comparison. 5 ml of 0,1% alcohol solution of resorcin was placed into the measured flask capacity of 25 ml. Then 5 ml of water was added into the flask. The volume of solution was led up to mark of 30% a hydrochloric acid solution, and it was mixed. Flask contents were poured into the test tube and heated up on the water bath at temperature 80 °C within 20 minutes, and cooled at room temperature. Optical density of the solution under the test was measured on the spectrophotometer at wave length of 480 ± 2 nanometers in a cuvette with thickness of a layer of 10 mm concerning a comparison solution.

The content of fructosides in conversion on fructose and absolutely dry raw materials in percentage $(X_1)$ was computed by the formula:

$$X_1 = \frac{D \cdot 200 \cdot 100 \cdot 100}{95 \cdot 1 \cdot 10 \cdot m \cdot (100 - W)} = \frac{0.131 \cdot 200 \cdot 100 \cdot 100}{95 \cdot 1 \cdot 10 \cdot 1 \cdot (100 - 3)} = 2.8432\%, \quad (2)$$

$$X_2 = X - X_1 = 86.5763\%$$

From the carried out researches it is possible to conclude that in powders obtained from topinambour tubers contains natural inulin polysacharide more than 86%.

Purified inulin has been obtained from the powder of topinambour tubers by dissolution last in hot water with the subsequent sedimentation of inulin from an aqueous solution with acetone addition in the ratio 1.0 : 1.0. In process of acetone addition (within 15–20 minutes) the white voluminous powder which to precipitated cooling at temperature 5–10 °C within 4 hours starts to fall out. Then the residue was separated by filtration, washed out with acetone, exsiccated, powdered and passed through a

sieve with diameter of apertures 0,1 mm. Obtained inulin was subjected to various physical and chemical analyses [5; 6].

Obtained easy-loose powder possesses humidity 7.0–8.0%, unlike starch it is not colored by an iodine solution, does not rebuild in Fehling liquid. Under resorcin effect and hydrochloric acid it is coloured in red colour (Selivanov reaction). In strong-acid medium inulin and polysacharide are completely hydrolyzed to monosaccharides. The generated fructose under the influence of temperature turns on 5 – hydroxymethylfurfural and it reacts in strong-acid medium with two molecules of resorcin. As a result of reaction the substance of red colour 9 – (5 – hydroxymethylfurfural – 2), 3 – ho, 6 – hydroxyxanthene [7], on the following mechanisms is produced.

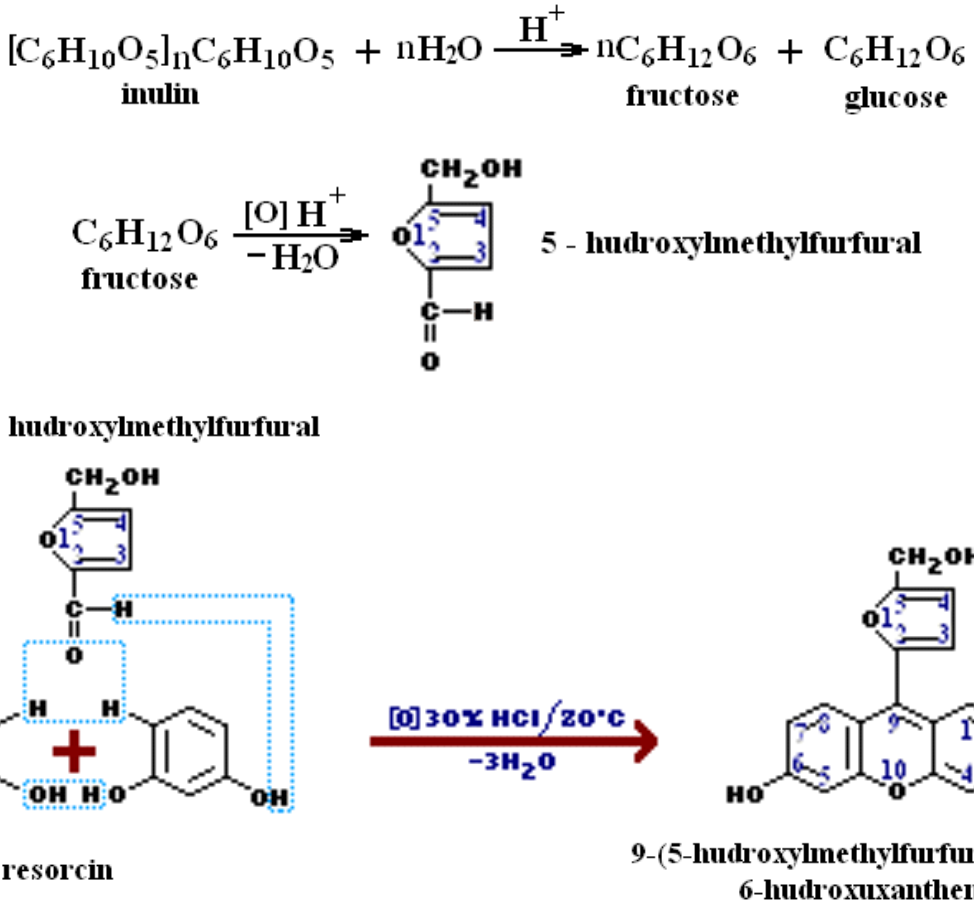


At TCX (dissolvent – ethanol, developer – 20%-s' alcohol solution of thymol and the diluted sulphuric acid) on a plate after drying at temperature 100–105 °C a brown-red stain with Rf = 0.75, characteristic for inulin.

## References:

1. Государственная фармакопея СССР.– X изд.– М.: Медицина, 1980.– 17 с.
2. Государственная фармакопея СССР.– XI изд.– М.: Медицина, 1987.– Вып. 1.
3. Кадиров О. Ш. и др. Стандартизация субстанции гликоинувита // Сб. тез. докл. науч. конф. молодых ученых, посвящ. 90-летию со дня рожд. проф. М. А. Азизова.– Ташкент, 2003.– С. 60–61.
4. Беляков К. В., Попов Д. М. Определение инулина в корневищах и корнях девясила высокого// Фармация.– № 1. 1998.– С. 34–35.

5. Багировой В. Л., Северцова В. А. Настойки, экстракты, эликсиры и их стандартизация / Под ред. В. Л. Багировой, В. А. Северцова / СПб.– Спец Лит., 2001.– 223 с.
6. Пономарев В. Д. Экстрагирование лекарственного сырья.– М: Медицина, 1976.– 204с.
7. Справочник химика.– Том 2. 1964.– С. 360–362.

# Section 6. Biotechnology

https://doi.org/10.29013/AJT-22-9.10-46-49

*Azizbek Bektemirov,*
*PhD student of Namangan Institute of Engineering and Technology, Uzbekistan.*
*Makhammadjon Soliev,*
*Head of the Chemistry Department of the Namangan Institute of Engineering and Technology, Uzbekistan.*
*Farkhod Hoshimov,*
*Professor of Namangan Institute of Engineering and Technology, Uzbekistan.*

## BIOLOGICAL EFFICIENCY OF ENTOLICUR FUNGICIDE AGAINST YELLOW AND BROWN RUST OF WINTER WHEAT CROPS

**Abstract.** The biological effectiveness of the fungicide Entolicur 22.5% a.e. was determined. LLC "Ifoda Agro Kimyo himoya" (Uzbekistan) with active ingredients (tebuconazole, triadimefon) to combat rust diseases and fusoria on winter wheat crops in the conditions of irrigated lands of Andijan region in 2022. The effect of the fungicide on growth and development, as well as on the yield of winter wheat, was studied.

**Key words:** fungicide, yellow rust, leaf rust, winter wheat, entolicur, tebuconazole, triadimefon.

**Introduction**

The increase in grain production in Uzbekistan should be ensured, first of all, by increasing the yield. To do this, it is necessary to use all available reserves. In the conditions of modern intensive farming, weed control is one of the most important elements of the farming system, on which the increase in crop yields depends. The results of research and the best practices of practitioners show that none of the factors of intensification of agriculture, except for special ones, aimed directly at combating diseases and pests, does not help reduce the harmfulness and reduce the weediness of fields.

Agricultural production currently has a significant range of fungicides, insecticides and herbicides to combat diseases, pests and weeds in the cultivation of crops.

**Materials and methods**

The criterion for the effective use of plant protection chemicals is the achievement of a given degree of suppression of harmful objects with minimal danger to human health and the environment. However, world experience shows that the constant and large-scale use of narrow-spectrum chemicals leads to a sharp increase in resistant insects to insectoacaricides, phytopathogenic to systemic fungicides, weeds to constantly used herbicides.

A high and stable grain yield can be obtained through the intensification of its cultivation. The

essence of this technology lies in the placement of culture ac-cording to the best predecessors, balanced plant nutrition and an integrated plant protection system. In solving this global problem, an important place belongs to the search for and introduction of new selective pesticides. The economic justification for their use will be determined by the amount of increase in the yield of grain crops.

In increasing the yield of grain crops, an important place belongs to the pro-tection of plants from diseases, which often lead to a significant reduction in grain harvest and deterioration in its quality, and sometimes to the death of crops. The degree of harmfulness of diseases depends on the environmental conditions of cul-tivation and the characteristics of the culture. In some ecological and geographical zones of the country, some diseases are more harmful, in others, others.

**Result and discussion**

It should be noted that, in the experimental plot in 2022, no Fusarium disease was detected before and after wheat treatment. Until the time of treatment with the fungicide Entolicur 22.5% a.e. (05/05/2022) the average total infestation of winter wheat crops with yellow rust in the test area was 28.6–29.8%, and the developed intensity was 16.2–17.1% (Table № 1).

Table 1. — Yellow rust infestation of winter wheat and intensity of disease development before treatment (May 5, 2022)

| № | Experience options | Consumption rate, l/ha | The total number of accounting plants per 1 sq.m. | Afflicted | | The intensity of the development of diseases, % |
|---|---|---|---|---|---|---|
| | | | | PCS. | % | |
| 1. | Control | No | 419 | 119,7 | 28,6 | 16,2 |
| 2. | Entolicur 22.5% a.e. | 0,3 | 420 | 120,2 | 28,6 | 16,2 |
| 3. | | 0,5 | 415 | 123,7 | 29,8 | 17,1 |
| 4. | Kolosal 25% (reference) | 0,5 | 423 | 119,5 | 28,3 | 16 |

According to the records and observations after treatment after 20 days with the fungicide Entolicur 22.5% a.e. in the control, where no fungicide treatment was carried out, the incidence of yellow rust reached 77.6% with a disease development rate of 90%. As a result of the treatment of diseased plants with the drug at a rate of 0.3 l/ha, the incidence was 17.5% and the intensity of disease development was 9.2%, in the variant where the drug was used at a consumption rate of 0.5 l/ha, the incidence was disease development 7.5%. In the reference variant, where the fungicide Colosal 25% a.e. was used. this indicator is 15.9–8.0%, which ensured the protection of the crop from losses due to the suppression of yellow rust.

The biological effectiveness of the fungicide Entolicur 22.5% a.e. in two test norms 0.3–0.5 l/ha was higher compared to the Colosal standard 25% a.e. drug Entolicur 22.5% a.e. in two test norms, it showed biological effectiveness (in terms of the intensity of the development of the disease) for yellow rust 77.4–80.4% and the standard 79.5%.

Infection and intensity of development of winter wheat brown rust were low compared to yellow rust before fungicide treatment, the infestation ranged from 17.9–18.4%, and the intensity of disease development was from 7.5–8.0%.

From the data of table 2 and 3, 20 days after treatment with the fungicide Entolicur 22.5% a.e. in the control variant without treatment, the incidence was 77.7%, and in the variants with the use of Entolicur 22.5% a.e. at a rate of 0.3 l/ha, the biological efficiency was 79.9%, and the intensity of the disease development was 7.2%. In the experimental vari-

ant, where Entolicur 22.5% a.e. was used. 0.5 l/ha biological efficiency was 83.5%, and the intensity of disease development was 6.7%. Almost on the same level with the reference variant, where Kolosal 25% a.e. was used. with a consumption rate of 0.5 l/ha, the biological efficiency was 80.9% and 7.0%.

Table 2. — Infection of winter wheat and the intensity of the development of the leaf rust disease before treatment with a fungicide (May 5, 2022)

| № | Experience options | Consumption rate, l/ha | The total number of accounting plants per 1 sq.m. | Afflicted | | The intensity of the development of diseases, % |
|---|---|---|---|---|---|---|
| | | | | PCS. | % | |
| 1. | Control | No | 419 | 70 | 16,7 | 7 |
| 2. | Entolicur 22.5% a.e. | 0,3 | 420 | 75,3 | 17,9 | 7,5 |
| 3. | | 0,5 | 415 | 76,2 | 18,4 | 8,0 |
| 4. | Kolosal 25% (reference) | 0,5 | 423 | 71,7 | 17,0 | 7,2 |

Table 3. — Biological efficiency and intensity of development after treatment with a fungicide against leaf rust on winter wheat (May 25, 2022)

| № | Experience options | Consumption rate, l/ha | The total number of accounting plants per 1 sq.m. | Afflicted | | The inten-sity of the development of diseases, % | Biological efficiency, % |
|---|---|---|---|---|---|---|---|
| | | | | PCS. | % | | |
| 1. | Control | No | 419 | 325,5 | 77,7 | 89,2 | |
| 2. | Entolicur 22.5% a.e. | 0,3 | 420 | 65,7 | 15,6 | 7,2 | 79,9 |
| 3. | | 0,5 | 415 | 53,2 | 12,8 | 6,7 | 83,5 |
| 4. | Kolosal 25% (reference) | 0,5 | 423 | 62,7 | 14,8 | 7 | 80,9 |

Thus, the results of the production test give us reason to conclude that the drug Entolicur 22.5% a.e. has high fungicidal activity and high biological efficiency against a complex of leaf diseases on winter wheat crops, like yellow and brown rust.

**Conclusions**

1. Field trials of the fungicide Entolicur 22.5% a.e. LLC "Ifoda Agro Kimyo himoya" (Uzbekistan) against leaf diseases like yellow and brown rust on winter wheat crops in irrigated lands of Andijan region with a consumption rate of 0.3 and 0.5 l/ha contributed to a decrease in the number of diseased plants with yellow rust on average by 77.4–80.4%, and brown rust by 79.9–83.5% and gave an increase in yield on average 1.1–1.9 q/ha compared to the control variant without treatment.

2. We believe that the use of the fungicide Entolicur 22.5% a.e. LLC "Ifoda Agro Kimyo himoya" (Uzbekistan) with a consumption rate of 0.5 to 1.0 l/ha is effective against leaf diseases in winter wheat crops under irrigated conditions in the Andijan region.

3. Taking into account the biological effectiveness of the fungicide Entolicur 22.5% a.e. and analogy D.V. with fungicide in the studied standard variant fungicide Colosal 25% a.e. we recommend including it in the list of the State Chemical Commission for the protection of winter wheat crops on irrigated lands from yellow and brown rust in the studied norms of 0.3–0.5 l/ha.

## References

1. Dikusar E. A. Synthesis and study of the fungicidal activity of amine salts of glycyrrhizic acid // Chemistry and vegetable raw materials. – 2011. No. 4. P. 53–56.
2. Soliev M. I., Abdilalimov O., Nurmonov S. E. The reaction for obtaining 3-vinyloxymethyl-chamazulene // Universum: chemistry and biology: electron. scientific magazine 2020.1(79). URL: https://7universum.com/en/nature/ archive/item/11051 (date of access: 09/26/2022).
3. Kazemi Mohsen. Chemical Composition and Antimicrobial Activity of Essential Oil of Matricaria recutita. International Journal of Food Properties. – 2014, № 18. P. 1784–1792.
4. Soliev M. I., Abdilalimov O., Nurmonov S. E. Technology for the production of vinyl esters of menthol and thymol // Universum: technical sciences: electron. scientific magazine 2021.9(90). URL: https://7universum.com/ru/tech/archive/ item/12254 (accessed 26.09.2022).

https://doi.org/10.29013/AJT-22-9.10-50-52

*B. Abdullaeva,*
*Namangan Institute of Engineering and Technology, Uzbekistan.*
*M. Soliev,*
*Namangan Institute of Engineering and Technology, Uzbekistan.*
*S. Nurmanov*
*National University of Uzbekistan, Uzbekistan.*

# ANTIOXIDANTS AND SYNERGISTS USED IN MEAT PRODUCTS

**Abstract.** This article talks about antioxidants and their enhancers, types and properties used in the production of minced meat semi-finished products and to extend their shelf life. Natural and synthetic additives with antioxidant properties, their use and benefits in various meat products are also reviewed.

**Keywords:** meat products, semi-finished products, food additives, fats, antioxidants, synergists, E-index, oxidation.

**Introduction**

Oxidation of fat components in meat products is one of the current problems of the meat processing industry. Oxidation processes reduce the nutritional value of meat products by changing the chemical composition of fats (liberation of fatty acids, formation of peroxides and secondary oxidation products) and by reducing the amount of fat-soluble vitamins (A, D, E, biotin, carotenoids). Free fatty acids, carbonyl compounds, alcohols and other secondary products of oxidation give an unpleasant taste and smell, have a negative effect on the quality of the finished product and shorten its shelf life.

Today, the list of antioxidants and their synergists used in the meat industry is much larger and they are defined by 42 E-indexes [1, 2].

Antioxidants used to prevent oxidative damage can be divided into two groups — synthetic and natural.

**Materials and methods**

Many synthetic substances can be cited as synthetic antioxidants: phenol derivatives (E 310–313, E 319–321), isoascorbic (erythorbic) acid (E315) and sodium isoascorbate (erythorbate) E316, E310–312 gallates. The most common in the world are butyloxyanisole (BOA or VNA) E320, butyloxytoluene (BOT or VTN) E321 and tert-butylhydroquinone (TBGX or TBHQ) E 319. These substances are soluble in oil and insoluble in water and can effectively resist the oxidation process of oil components (concentration is 20–200 mg per 1 kg of product). But this compound has no nutritional value, besides its carcinogenic effect on living organisms has been proven. For this reason, humanity is abandoning synthetic additives and turning to natural antioxidants that are harmless to health. Also, natural antioxidants have biological value.

Synthetic antioxidants such as BOA, BOT, DG are considered phenolic inhibitors and stop oxidation processes under the influence of peroxide radicals or have a synergistic effect with natural antioxidants. In contrast to the mentioned antioxidants, the antioxidant activity of ascorbic acid is related to its ability to return natural and synthetic antioxidants to their initial form due to the interruption of the hydrogen atom in it [3].

Antioxidants slow down oxidation processes by interacting with air oxygen (blocking air oxygen from reacting with the product), stopping oxidation reactions in the product (blocking active radicals)

or breaking down peroxide compounds that have been formed. In this case, the antioxidant substances themselves are used up. In addition, antioxidants can be conditionally divided into two more groups: real and secondary. Real antioxidants interact with air oxygen, slow down oxidation processes (block the effect of oxygen on the product), deactivate active radicals, interrupt oxidation reactions, or decompose the peroxides formed. Secondary antioxidants affect the product's redox potential, activity, and water in the product. Secondary antioxidants can be both antioxidant and oxidant depending on the dose. For example, ascorbic acid in a small amount (up to 200 mg/kg) slows down oxidation, and when its amount is increased to 5000 mg/kg, it has an oxidizing effect on the product. An unlimited increase in the dose of real antioxidants does not extend the protection time of the product. In practice, a threshold concentration is established for most antioxidants, beyond which the shelf life of the product will not be extended [4].

There is little information on the permissible limit concentration of peroxides and hydroperoxides in food products. The use of antioxidants to eliminate the oxidation of fatty products is of particular practical importance. Because such products undergo a high degree of oxidative destruction during extraction, processing and storage [2].

Many types of synthetic and natural antioxidants are used worldwide. The antioxidant activity of compounds depends on the nature of the product and a number of factors. Therefore, it is necessary to conduct scientific research to justify the effect of antioxidants and their complexes on specific food products [3].

Natural antioxidants found in plants and foods include: flavanoids (flavone, flavonol, flavonone, isoflavonone, flavononol, flavan, chalcone, dihydrochalcone, flavone-3,4-diol, anthocyanidins); benzoic acid derivatives (gallic, protocatechin acids, vanillin, sirenic acids); cinnamic acid derivatives (ferulic acid, para- and ortho-coumaric acid, caffeic and sinanic acids); coumarin derivatives; phytoestrogens (lignans, estrogens, lactones, etc.); vitamins: vitamin E (a, b, g, d-tocopherols and a, b, g, d-tocotrienols), vitamin C; carotenoids (lycopene, α, β-carotenes, lutein, etc.) [5].

**Result and discussion**

Spices, various oils, tea, seeds, grains, cocoa pods, fruits and vegetables are used as natural antioxidants. The antioxidant activity of natural compounds containing various individual antioxidants such as ascorbic acid, tocopherols, carotenoids, as well as flavonoids (quercetin, kaempferol, myricitin), catechins or phenols (carnosol, rosmanol, rosamiridiphenol) and phenolic acids (carnosine, rosemary) has been proven [6, 7, 8]. In particular, it was found that the activity of essential oils of anise, cumin, Indian basil, peppermint is stronger than the synthetic antioxidant butyloxytoluene in sunflower oil, and the oil of Ayovan (cumin) is almost 2 times more effective (Table 1).

Table 1. — Antioxidant activity of essential oils in sunflower oil

| The name of the essential oil | Peroxide number of sunflower oil, mg-equiv | |
|---|---|---|
| | After 7 days | After 14 days |
| Control | 86.3 | 581.0 |
| Butyloxytoluene | 51.2 | 418.5 |
| Anise oil | 40.6 | 238.2 |
| Cumin oil | 42.2 | 312.4 |
| Peppercorn oil | 41.0 | 248.2 |
| Indian basil oil | 46.2 | 302.5 |
| Iowan oil | 32.2 | 229.5 |

E 306–309 tocopherols are natural fat-soluble antioxidants found in vegetable oils. All tocopherols, except natural tocopherol extract E 306, are obtained synthetically in industry. These substances show different levels of vitamin E activity, but 8-tocopherol E 309 has the highest antioxidant activity [9].

The use of individual antioxidants does not always allow to protect the product from oxidative deterioration. Therefore, it is advisable to use several antioxidants together. In this case, a synergism phenomenon occurs, and the combination of several (usually 2) antioxidants increases their antioxidant capacity. For example, when ascorbic acid is added to the mixture of tocopherols in the production of meat products, the efficiency increases significantly [10].

The effect can be enhanced by mixing substances that do not have an antioxidant effect or are weak antioxidants with antioxidants. Such synergistic substances include some polybasic organic oxyacids (citric acid E 330), a number of amino acids, polyphosphates, EDTA and other compounds.

Oils and fats have different natural stability against oxidation according to the structure of fatty acids, as well as the presence of natural antioxidants such as tocopherols, tocotrienols, carotenoids, phospholipids. The natural stability against oxidation is expressed by multiplying the number of unsaturated acids in the oil (in decimal form) by its relative oxidation rate and adding the value of this rate to the obtained number.

## References


1. GOST 9957–73. Meat products. Methods for the determination of sodium chloride [Text]. – M.: Gosstandart, 1974. – 4 p.
2. GOST 9959–91. Meat products. General conditions for organoleptic evaluation [Text]. -M.: Publishing house of standards, 1991. – 20 p.
3. GOST 26932–86. Raw materials and food products. Lead determination method [Text]. M.: Publishing house of standards, 1990. –11 p.
4. D.L. Bozhko, SV. Radkov. Measurement of water activity as one of the criteria for assessing the shelf life of meat products [Text] // Food industry: science and technology. 2008. No. 1. -S. 79–82.
5. Gurinovich G. V. Preparation for extending the shelf life of semi-finished meat products [Text] / G.V. Gurinovich, K.V. Lisin, N.N. Potipaeva // Meat industry; – 2005. – No. 2. – S. 31–33.
6. Gutnik, B.E. On the state of the meat industry in Russia [Electronic resource] / B.E. Gutnik. – II International Investment Forum «Strategy for the development of the food industry and investment in food production in times of crisis.» Within the framework of the 14th International Exhibition «Agroprodmash-2009», October 14, 2009 Site materials http://www.agromg.ru/events/.
7. Dorozhkina T. P. Natural antioxidants for mayonnaises and dressings [Text] / T.P. Dorozhkina // Oil and fat industry. –2009.- № 4. -FROM. 26–27.
8. Dotsenko S. M. Semi-finished products from minced meat and vegetables [Text]. / CM. Dotsenko, O.V. Skripko SN. Parfenova // Meat industry. – 2005. – No. 2. -FROM. 28–30. (13)
9. Sharygina Ya.I. Improving the technology of minced meat semi-finished products using natural substances with antioxidant properties // dis. candidate of technical sciences: 05.18.04 / – Kaliningrad, 2011. – 165 p.
10. Abdullaeva B. T., Soliev M. I. Determination of antiradical activity of wormwood and pine extracts // Universum: chemistry and biology: electron. scientific magazine 2021.9(87). URL: https://7universum.com/en/nature/archive/ item/12245 (Accessed: 03/04/2022).


11. Bufotima Abdullaeva – PhD student of Namangan Institute of Engineering and Technology e-mail: bufotima@gmail.uz, phone: +99888–688 1990.

12. Makhammadjon Soliev – Head of the Chemistry Department of the Namangan Institute of Engineering and Technology, e-mail: muhammadbey@mail.ru. tel. +99897–410–7006
13. Suvankul Nurmanov – Professor of National University of Uzbekistan, e-mail: nurmonov_se@mail.ru. +99890–990–8483.

# Contents